University of Stavanger

Faculty of Science and Technology

MASTER'S THESIS

Study program/Specialization: Petroleum Engineering/ Natural Gas Engineering	Spring semester, 2016 Open
Writer: Marta Øvstebø	…… (Writer's signature)
Faculty supervisor: Rune W. Time Hermonja A. Rabenjafimanantsoa	
Thesis title: Development of a Thermal Based Flow Measurement Technique for Very Low Flow Velocities	
Credits (ECTS): 30	
Key words: Flow measurement Cross correlation Heat flow dynamics PIV, high speed recording	Pages: 81 + enclosure: 16 Stavanger, 15.06.2016

Acknowledgement

The work with this thesis was performed in the multiphase laboratory for the Department of Petroleum Engineering at the University of Stavanger. As a part of my work I would like to thank the following people:

Professor Rune W. Time, who gave me the opportunity to write an experimental thesis that I thought was very interesting, for good guidance and comments, and for providing MATLAB programs used in data analysis.

Senior Engineer Hermonja A. Rabenjafimanantsoa, Benja, for sharing his enthusiasm of working in the laboratory, for providing good guidance and assistance throughout this process and for the feedback during the writing of this thesis.

I would like to thank Olav Øvstebø and Annbjørg Fiveland for helping with proof-reading and feedback. And at last I would like to thank my family and friends who have supported and encouraged me while working on this thesis.

Marta Øvstebø

Abstract

A measurement technique for very low flow velocities based on thermal measurements is proposed as an alternative for measurements in larger-diameter pipes. The velocity of a locally accelerated thermal flow is calculated from the time shift between registration of heat pulse and distance separating the two temperature sensors. Additional study using PIV and high-speed recording in analysing and quantifying the flow pattern induced by heat pulses in static and dynamic environments is performed.

The results from this study showed that a clear and distinct registration of heat pulses was necessary in order to easily calculate the average velocity. Based on small-scale laboratory works, location of the measurement equipment was decisive in terms of getting best possible registrations of heat pulses. The results show a jet-like pattern of the movement induced by heat pulse in static environment and the collision of jets resulting in a mushroom-like vortex structure in the dynamic environment.

Nomenclature

Abbreviations

THC	Thermohaline Circulation
NADW	North Atlantic Deep Water
PIV	Particle Image Velocimetry
FPS	Frames per second
CLAHE	Contrast-limited adaptive histogram equalization
TLC	Thermochromic liquid crystals

Greek letters

σ	Stefan-boltzmann constant $[W/m^2]$
ϵ	Emissivity
μ	Viscosity $[Ns/m^2]$
ρ	Density $[kg/m^3]$
σ	Standard deviation
ρ_w	Density of water $[kg/m^3]$
C_pw	Specific heat capacity [J/gC]
τ	Transit time [s]

Roman letters

A	Area [m^2]
A_m	Velocity magnitude [m/s]
A_s	Surface area [m^2]
D	Diameter [m]
D_p	Pipe diameter [m]
E	Energy [J]
H	Height [m]
H_l	Air level [cm]
I	Current [A]
I_n	Turbulence intensity
k	Thermal conductivity [W/mK]
L	Distance [m]
$\bar{L}$	Particle displacement [m]
m	Mass [g]
P	Power [W]
Q	Flow rate [m^3/s]
Q_h	Rate of heat transfer [W/m^2]
q	Heat [J]
$\dot{Q}$	Rate of radiation [W/m^2]
R	Radius from centerline to the pipe wall [m]
r	Distance from pipe center [m]
Re	Reynolds number
Rxy	Cross correlation function
S_1	Sensor 1
S_2	Sensor 2
T	Number of measurements
t	Time [s]
$\frac{dT}{dx}$	Temperature gradient [K/m]
T_S	Surface temperature [K]
T_{surr}	Temperature surroundings [K]

T_0	Observation period [s]
U	Average flow velocity [m/s]
U_v	Voltage [V]
u(r)	Velocity profile [m/s]
Uavg	Average flow velocity [m/s]
Umax	Maximum velocity [m/s]
u	Velocity in x-direction [m/s]
$\bar{u}$	Mean velocity in x-direction [m/s]
$u'(t)$	Turbulent fluctuations in x-direction
u_t	Average value in moving averages
U_{rms}	Root mean square of turbulent velocity fluctuations
V	flow velocity [m/s]
v	Velocity in y-direction [m/s]
$\bar{v}$	Mean velocity in y-direction [m/s]
$v'(t)$	Turbulent fluctuations in y-direction
v_t	Neighbouring values in moving averages
V_p	Volume [cm^3]
$\bar{V}$	Velocity vector

Table of Contents

List of Figures

List of Tables

Introduction

Measurement of flow rate is important in many different disciplines today: medicine, industry, food production, surveillance and laboratories to mention some. A wide variety of flow rate measuring methods has been developed, based on different principles. Even so, accurate flow rates in units down to cm^3/s is difficult to detect with the existing flow meters. There is a need for new ways to measure low flow rates in large-diameter pipe. A flow meter measuring low flow velocities in pipes with larger diameter that can detect small changes in flow rate with high precision can provide an even better insight of the fluid flow in pipes. Such a flow meter could be used for early detection of changes in flow velocities e.g. in relation to leakage detection.

The objective in this thesis is to develop a method for measuring very low flow velocities in pipes. Along developing a measuring method it is also desirable to test equipment from Pasco and its area of application. This is an experimental study performed in the multiphase laboratory at the University of Stavanger.

The measurement method is based on sending thermal pulses into a fluid and by registering the heat pulse at two different locations along the pipe, being able to calculate the flow velocity. Cross correlation is chosen as method for finding the difference in time, Δt, for which the thermal pulse reaches the two points, the time shift is seen in figure 1.1. In order to develop the method a vertical and horizontal experimental setup are built.

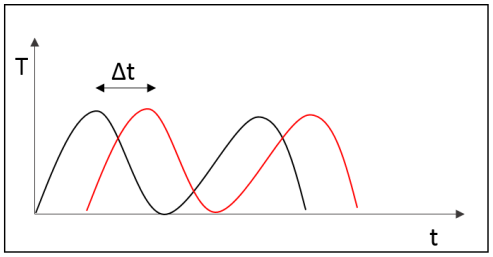

Figure 1.1: Cross correlation analysis

A motivation for this thesis is a collaboration project called the NORTH project. The name NORTH has its origin in northern constraints on the Atlantic thermohaline circulation. The project is a collaboration with the Bjerknes Centre and the University of Stavanger among others. The University of Stavanger involvement in this research project so far has been to build an experimental model of the thermohaline circulation. The thermohaline circulation is the ocean circulation driven by differences in density and salinity. This thesis is a preliminary study in relation to the NORTH project.

This thesis is purely experimental. The development of a measurement method is described. The thesis is organized starting with theory related to the experiments in chapter 2, detailed description of the experimental setup and procedures in chapter 3, results and discussion based on experiments performed is presented in chapter 4 and ends with a part which concludes the development of measuring method.

Theory

In this chapter a short introduction of some topics relevant in developing the measurement technique is given. Among these topics are the NORTH thermohaline project, fluid flow in pipes, principles of measurement and Particle Image Velocimetry.

2.1 Flow Measurements

Flow measurements can be divided into non-thermal and thermal. The non-thermal methods widely used today measure the flow rate indirectly by means of e.g. drag force, pressure differences or vortex shredding. One example is the Coriolis flowmeter, which measure the change in oscillations of fluid passing through an oscillating tube. This instrument is one of the more accurate non-thermal flowmeters. The thermal methods for measuring flow are often divided into three main types:

- Hot- wire and hot film flowmeters
- Calorimetric flowmeters
- Time-of-flight flowmeters

Measurement methods like these are intrusive i.e. invading the flow as it measures. The thermal flowmeters that measures how the flowing fluid affects a hot body maintaining its constant temperature, is called hot-wire and hot-film flowmeter. The calorimetric flowmeters consist of heating element and temperature sensors. These flowmeters measure the asymmetry of temperature profil around the heater. The time-of-flight flowmeters measure the passage of time of a heated pulse over

a known distance [5].

The flow velocity can be measured using active or passive sensors. The difference between these principles is the way input is registered. Active meters emits energy that is modified by moving objects, e.g. electromagnetic waves used in Doppler meter reflects the energy with a frequency describing whether the object is moving away or towards the observer. A passive sensor measures the time needed for an object to move between two positions with a known distance between them [6]. A cross correlation technique can be used to find the difference in time for the object to pass from one position to the other, in section 2.5.4 a more detailed description of this technique is described.

2.2 The NORTH Thermohaline Project

The NORTH project is a collaboration between the University of Stavanger, Woods Hole Oceanographic Institute, University of Washington, Danmarks Metrologiske Institut, Finnish Metrological Institute and the Bjerknes Centre [7]. The research project is initiated to assess the fundamental structure and operation of the Atlantic thermohaline circulation's northern limb. Finding its constraints in mean state, variance and sensitivity, and relate the results to observed and projected climate change.

In parallel to this research, the University of Stavanger is constructing and developing an experimental model of the thermohaline circulation. The experimental setup, called the NORTH loop, is based on the Stommel's model and is a 4.5 m vertical system. Water with variation in temperature and salinity will flow through the experimental system to simulate the ocean circulation [7].

The NORTH Loop

The construction is made of two vertically placed pipes of transparent acrylic with a length of 4.5 m and an inner diameter of 5.0 cm. At the bottom and a half meter from the top of the two pipes, passages are placed across so that the working

fluid can circulate and the overturning can happen. A system which is feeding water with variation of temperature and salinity into the system, is connected to the pipes. The differences in temperature and salinity represents water from the different latitudes.

2.2.1 Thermohaline Circulation

The ocean circulation is divided into surface circulation and the thermohaline circulation(THC). The surface circulation is surface currents from wind and tides which appears in the upper part of the oceans. The thermohaline circulation is the part of the ocean circulation which involves deep water circulation. These two circulations interact with each other and together they represent the ocean circulation.

The thermohaline circulation is a term used to describe how the ocean circulation is mostly driven by differences in density. The term is directly inspired from temperature in thermo- and from salinity in the haline, since the density varies as a function of salinity and temperature of the water. The difference in density controls the direction of flow and overturning of the oceans.

The circulation happens in a way that the warmer surface water in areas near Equator drifts north towards the Arctic Ocean, in these cold regions the water achieves the highest surface water densities. The high densities causes the surface waters to sink and become deep water. The already existing deep water in the Arctic Ocean, that is replaced, has to circulate away. This circulation takes place by turbulent mixing in the ocean's interior. The turbulence which causes the mixing is powered by winds and tidal motions. The upwelling of the deep waters drives the water to southern latitudes.

The change in temperature and salinity is results of heating or cooling at sea surface and surface freshwater fluxes. The key features of THC is:

- Deepwater formation
- Spreading of deep water (e.g. North Atlantic Deep Water, NADW)

- Upwelling of deep water
- Near-surface currents

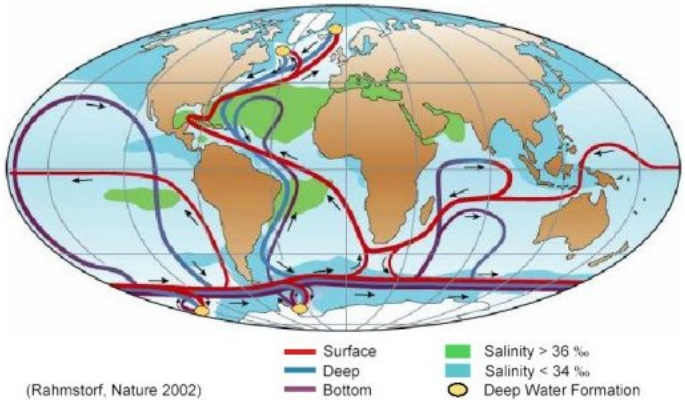

Figure 2.1: Illustration the global thermohaline circulation [1]

Figure 2.1 is an illustration of the thermohaline circulation, the surface currents are shown in red, deep waters in light blue and in dark blue the bottom waters. The yellow markers shows the sites of where the main deep water formation occurs [1].

2.2.2 Stommel's Model

A widely known model of the ocean circulation is the Stommel's model. Stommel(1961) developed a model with the purpose of visualizing the circulation in the oceans. The model consisted of two boxes filled with water, one representing the ocean of high-latitude the other one representing the ocean of low latitudes. The boxes were placed side by side and were connected with one tube at the top and another one at the bottom. The circulation between the boxes was through the tubes, on top the overflow and on bottom the capillary flow. The direction of the capillary flow was controlled by the density differences between the water in the two boxes. The two boxes had both a seperating wall with a storage tank providing salt or heat to the water in the box, by diffusion through the porous walls. The tank representing the tropical ocean had a storage tank containing hot salty water, while the box representing the polar region had a storage of cold fresh water. To ensure a uniform concentration as the fluid flowed between the two boxes, two mixing propellers were used. An illustration of Stommel's two box

model is shown in Figure 2.2. The Stommel model has laid the foundation for many similar models of ocean circulation in years after [2, 8].

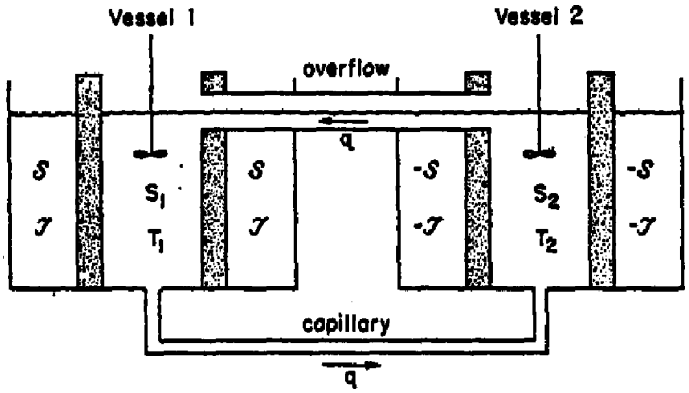

Figure 2.2: Illustration of Stommel two box model [2]

2.3 Heat Transfer

Energy exists in various forms, one of them is heat. Heat is produced when energy is transferred as a consequence to a temperature difference. The transfer is always between a system of higher temperatures to a system of lower temperatures. The rate of this kind of energy transfer is known as heat transfer. Heat transfer can be divided into three mechanisms: Conduction, convection and radiation, which will be presented in this section [9].

2.3.1 Heat Transfer in Fluids

Describing how a fluid reacts when a thermal pulse is applied involves several processes of heat transfer. Movement of the fluid due to a thermal pulse involves advection, diffusion and convection.

Advection is a transport mechanism where energy is transferred by the bulk fluid motion. One relevant example of advection is a heat pulse applied in a pipe with water flowing inside it. As the water flows, the thermal pulse will follow in the direction of the water via advection. However, while the thermal pulse flows with the water it will also spread via diffusion [10].

Diffusion is a process where difference in concentration is the driving force. The molecules or atoms in a region of higher concentration will move to a region of lower concentration, the net movement is diffusion. In comparison with advection, bulk motion is not required for diffusion to occur.

Convection: The moment a thermal pulse is sent and heat is transferred into the fluid, the heat flow will spread out into the fluid by advection in the direction fluid flows. In the same time, the heat will also be spread by diffusion. The transfer of heat due to convection covers both advection and diffusion. Convection is heat transfer between a solid surface and an adjacent fluid in motion. Convection is either forced or natural. If the fluid in a system is forced to flow by the means of an external source like pump or wind, it is defined as a forced convection. The system where the fluid flows naturally and only buoyancy forces affect is known as natural convection. Convection has a higher rate of heat transfer through a fluid in comparison to conduction; this is because fluid motion enhances heat transfer.

In a horizontal enclosure natural convection in the form of convective currents can occur. Currents like these is often called convective cell and occurs in situations where there exists difference in density within a body of liquid or gas. The difference in density is a result of heating and cooling. These differences results in a circular motion in the body, rising and/or falling currents. The heated fluid expends and becomes less dense than the surrounding fluid, because of this the fluid rises due to buoyancy forces. The colder fluid is denser and sinks and settles below the warmer fluid. This process continues and develops a body of the fluid which is in the form of hexagonal cells, known as a *Bénard* cell [9], seen in figure 2.3.

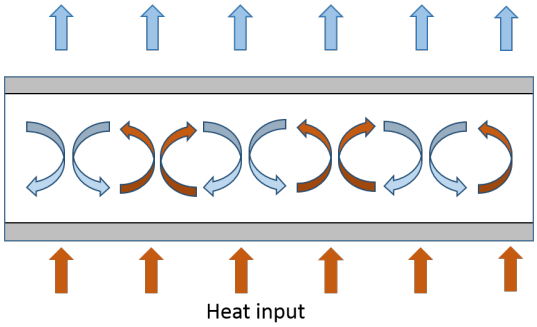

Figure 2.3: Illustration of convective currents

2.3.2 Heat Transfer in Matter

Conduction is the transfer of internal energy caused by interactions between particles that are more energetic and the adjacent less energetic particles in a substance. Such a heat transfer can occur in solids, liquids or gases. The rate of heat transfer is expressed in Fourier's law of conduction,

$$Q_h = -kA\frac{dT}{dx} \tag{2.1}$$

Which states that the rate, Q_h, is proportional to the thermal conductivity, k, the total area, A, and the temperature gradient, $\frac{dT}{dx}$. The thermal conductivity given in W/m K varies according to the ability for a substance to make the transfer. Highest values of conductivity is found for the metals, and in decreasing order it is the non-metallic solids, liquids and gases. Shown in the table below are the conductivity of some materials and gases [9, 11]

Table 2.1: Thermal conductivity of materials and gases [4]

Matter	Conductivity [W/mK]
Air	0.024
Water	0.58
Tungsten	174
Acrylic	0.2

2.3.3 Radiation

The last mechanism of heat transfer which also should be mentioned is radiation. Radiation is thermal energy emitted to the surroundings by the matter in the

form of electromagnetic waves. Radiation is the quickest way to transfer heat. It does not require the presence of a material medium to take place, compared to the two other mechanisms of heat transfer. Radiation occurs in different forms, but the radiation emitted by bodies because of their temperature is called thermal radiation. Thermal radiation is the form of radiation of interest here.
The rate of radiation emitted by a surface is given by the Stefan- Boltzmann law,

$$\dot{Q} = \epsilon \sigma A_s T_s^4 \tag{2.2}$$

where T_s is the surface temperature in K, $\sigma = 5.670 \cdot 10^{-}8 W/m^2 \cdot K^4$ is the Stefan-boltzmann constant, A_s is the surface area in m^2 and ϵ is the emissivity of the surface. Emissivity is a measure of how closely the surface is to a blackbody, which is an idealized surface that has the maximum rate of radiation. All real surfaces emits heat of a lower rate compared to a blackbody and the value of emissivity lies in the range of 0 to 1, in which 1 represents a blackbody.

The net rate of radiation heat transfer from a body to the surroundings is depending on the temperature of the surface of the body, T_s and the surroundings, T_{surr}. The relation is given [9],

$$\dot{Q} = \epsilon \sigma A_s (T_s^4 - T_{surr}^4) \tag{2.3}$$

2.4 Fluid Flow in Pipes

In single phase flow in pipes, the flow pattern of a fluid can be divided into laminar and turbulent flow. There exist a transitional zone between these flow patterns if one takes a closer look, but only a short description of the two main types will be presented in this section.

The Reynolds number, Re, is a dimensionless quantity used to characterize flow regimes. Re, which is based on the ratio of inertial forces to viscous forces, is used to differentiate between different flow regimes. The expression is given in equation 2.4,

$$Re = \frac{Inertial forces}{Viscous forces} = \frac{\rho U D}{\mu} \tag{2.4}$$

where ρ is the density of the fluid, U is the average flow velocity, D is the characteristic length of the geometry and μ is the viscosity of the fluid.

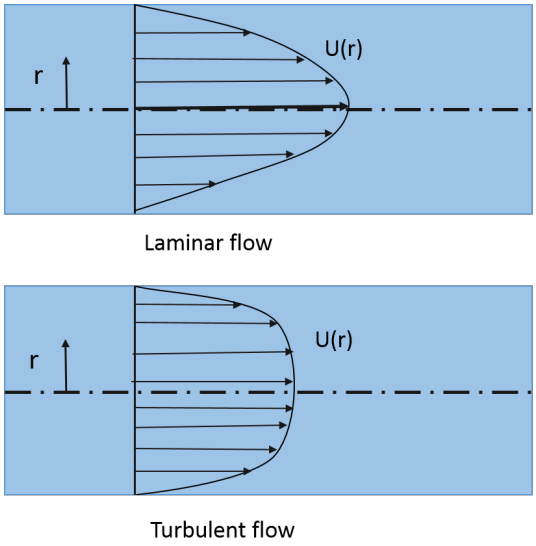

Figure 2.4: Flow profiles of fully developed laminar and turbulent flows

2.4.1 Laminar Flow

Laminar flow in pipes can be describes as flow following smooth streamlines in a highly ordered motion. For Re $<$ 2300 the flow in a circular pipe is defined as laminar.

The velocity profile of laminar flow is parabolic, see figure 2.4. The velocity in the axial direction is constant and there is no motion in the radial direction. For the steady and fully developed flow the velocity profile remains unchanged in the flow direction. The velocity profile u(r) of a laminar flow is expressed in equation 2.5.

$$u(r) = 2U_{avg}(1 - \frac{r^2}{R^2}) \tag{2.5}$$

Where the Uavg is the average velocity of the fluid flow, r is distance from pipe center and R is the radius from centerline to the pipe wall. The average velocity for a fully developed laminar pipe flow is half of the maximum velocity, $Uavg = \frac{1}{2}2Umax$.

2.4.2 Turbulent Flow

For high Reynolds numbers, Re > 4000, the flow regime is turbulent flow. Turbulent flow is characterized by highly disordered motion and velocity fluctuations. The disorderly and rapid fluctuations of swirling regions of fluid throughout the flow is called eddies [9, 12]. The velocity profile seen in figure 2.4 is much flatter or fuller, compared to the profile of laminar flow. This is due to more strongly mixing in radial direction and the eddy motions in turbulent flow. At a certain point in the fluid the actual flow velocity in two dimensional turbulent flow could be found about a mean value. Two-dimensional flow can be decomposed as follows:

$$u(t) = \bar{u} + u'(t) \text{ in the horizontal direction}$$
$$v(t) = \bar{v} + v'(t) \text{ in the vertical direction}$$

where $\bar{u}$ and $\bar{v}$ are the mean velocity and u'(t) and v'(t) are the turbulent fluctuations [13].

Turbulence Intensity

Turbulence intensity is a measure of turbulence level of a fluid flow. Turbulence intensity is defined in the following equation,

$$I_n = \frac{u_{rms}}{\bar{u}} \tag{2.6}$$

where the u_{rms} is the root-mean-square of the turbulent velocity fluctuations and $\bar{u}$ is the mean velocity [14].

2.4.3 One-dimensional Flow

Generally flows are three-dimensional but fluid flow in circular pipe can be studied as if they are one-dimensional. Fluid flow in circular pipe is one-dimensional if the velocity across the whole cross-section of a pipe has the same direction, and for an incompressible fluid magnitude is also the same. Such a flow is rarely of practical interest. However, the term one-dimensional method is applied in analysis to the flow between boundaries that are really three dimensional, with the understanding that the one 'dimension' is taken along the central streamline of the flow. By

doing so the average values of velocity, pressure and elevation across a section normal to this streamline is considered to be typical of the flow as a whole [15].

2.5 Principles of Measurement

While working with this thesis several principles of measurement were seen as relevant. In this section time series analysis, time constant, signals and cross correlation are explained.

2.5.1 Signals

A flowmeter or pressure transmitter is a transducer. Transducer is a device that receives a signal in the form of one type of energy and converts to a signal in another form.
Signals can be described as deterministic or random. For a deterministic signal the measured value at any future time can be exactly predicted, based on recordings of the signal for an observation period T_0. Two types of deterministic signals is step and sine wave signals. However, in real processes the signal can not be known in advance due to its dependency of unknown factors. The input signal is random and not deterministic. If a random signal is measured for an observation period T_0, the behaviour of the signal, once the period is over, is not known exactly [16].

2.5.2 Time Series Analysis

Analysis of experimental data often involve processing of time series. Data recorded in time series are either evenly spaced or unevenly spaces, a method to minimize the amount of data to be analysed is by moving averages, these principles will be presented here.

Evenly spaced time series: Experimental data recorded with a constant sampling rate, which has a time between each measured value equal to Δt is an evenly spaced time series.

Unevenly spaced time series: Analysis of experimental data that have been measured at different points in time needs adjustment to be able to be compared with data of even time series. A possible way to convert an uneven time series into an even one is by nearest neighbour-interpolation.

Moving averages: A method to make it easier to process the measurement data is by using moving average. By smoothing the time series one reduces the amount of data to process and achieve a more clear indication of the data. Moving average is done by replacing a value by the average of its current value, and its immediate neighbouring values in the past and the future, as given in equation 2.7.

$$u_t = \frac{1}{3}(v_{t-1} + v_t + v_{t+1}) \tag{2.7}$$

Equation 2.7 shows the general formula, where the average of three values are found, called three-point moving average. The amount of values one finds the average of is determined for each individual case, in relation to what kind of experimental data one is processing [17].

2.5.3 Time Constant

Time constant is the parameter used in physics and engineering to characterize the response. Response of sensor is the period of time that goes by from the moment a change of the input parameter occurs, until the moment the sensor has registered the change in the output state. If the time of response of a sensor is longer than the time scale of the process under study, certain features of the measured parameter could be partially or totally non-accessible to the sensor itself [18].

2.5.4 Cross Correlation

Estimation of time shift between the two temperature probes is calculated using cross correlation. The cross correlation function Rxy of two heat pulse signals S_1(t) and S_2(t) at sensors 1 and 2, is defined by equation 2.8 when heat pulses is sent out from the heat source.

$$R_{xy}(\tau) = \frac{1}{T} \int S_1(t) \cdot S_2(t+\tau) dt \tag{2.8}$$

The transit time τ is given by the τ at which the Rxy (τ) is maximum. The transit time is used for calculation of flow velocity in the pipe, where L is the distance between the sensors.

$$V = \frac{L}{\tau} \tag{2.9}$$

Further, the flow rate Q of the flow is given by multiplying the velocity with the cross-sectional area of the pipe [16].

2.6 Particle Image Velocimetry

PIV is an optical non-intrusive measurement technique with a wide variety of applications. There are several PIV measuring methods, the measuring method used in the experiment is time resolved PIV, conducted using a high-speed camera at a fixed frame [19]. Illustration of the measurement principles is shown in Figure 2.5.

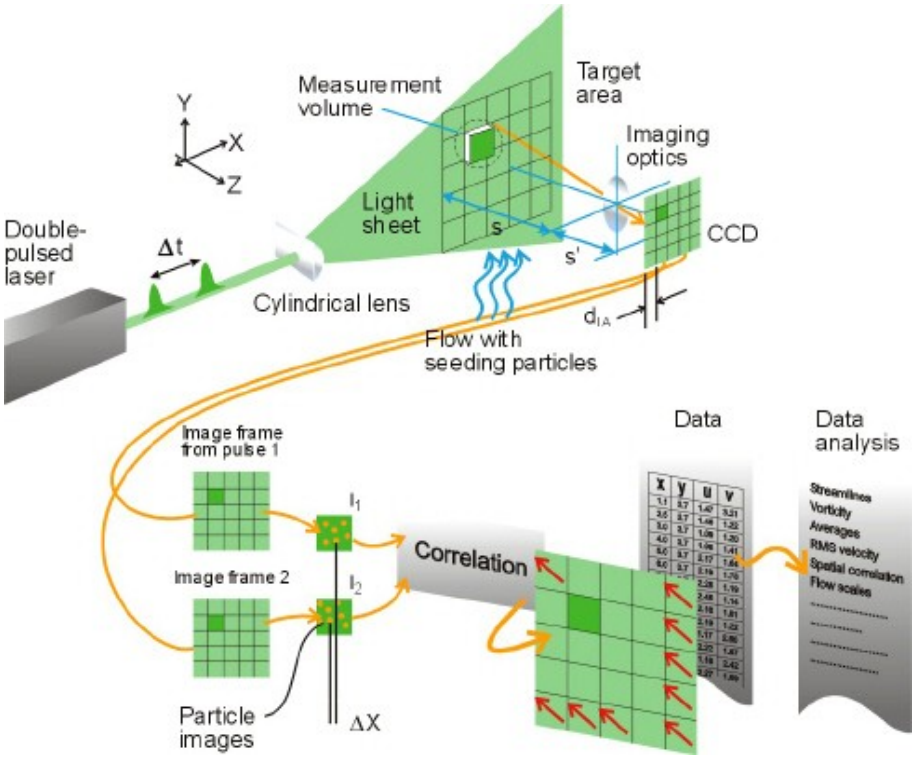

Figure 2.5: Measurement principles of PIV [3]

The principle of PIV is to measure the difference in movement of seeding particles injected into the fluid during a certain time lapse from which velocity vectors can be derived.

$$\bar{V} = \frac{\Delta \bar{L}}{\Delta t} \tag{2.10}$$

The fluid to be investigated is injected with seeding particles, this being done for it to be possible to see the flow directly in the homogeneous liquid. The area of interest of the flow is illuminated with a light sheet. A high-speed camera is used to record the flow of particles in the specific area. The recorded video is split into single picture frames, which is used for further analysis. In the analysis, the images are divided into small subsections called interrogation areas. The interrogation areas for each of the image frames are cross-correlated with each other. The correlation results in a signal peak, which indicates the common particle displacement, ΔL. An accurate measure of displacement is achieved with sub-pixel interpolation. When the cross-correlation analysis is executed on all frames, a velocity vector map over the whole target area is obtained [19].

2.7 Ball Valve Characteristics

Ball valve is a type of valve typically used for shutoff applications. The ball valve is a valve consisting of a spherical plug that controls the fluid flow through the valve body. This spherical ball has a orifice through its center, in which the fluid flows. The ball hole axis of the valve is controlled by a handle. The handle rotates from 0 to 90 degrees, from closed to fully opened. The ball valve is mostly used to shut off or on fluid flow, but a slight flow regulation is possible.

Several studies has been performed in order to estimate the performance of a ball valve. It is shown that the valve opening and the inlet velocity plays a vital role in the flow characteristics of a ball valve. For a not fully opened valve, three vortices is observed in the flow field, two inside the ball and one behind the exit of the ball valve. These vortices grows as the valve opening decreases, possibly causing more pressure drop. This way the flow is effected by the geometry of the valve and cavitation may occur. The opening of the valve also affects the energy dissipation behind the ball valve. At small valve openings, more energy is required to maintain the same volumetric flow rate or the same inlet velocity [20].

Experimental Method

The aim of the following experiments is to develop a thermally based measurement technique for low fluid velocities. The measurement technique is based on fast temperature measurements of thermal pulses applied to a flowing fluid in a pipe. Measurement equipment from Pasco is used for fast temperature measurements. By calculating the time shift between the heat pulse registration from two temperature probes and the measured distance between them, the mean velocity of the locally accelerated thermal flow can be calculated.

This chapter begins with a feasibility test describing a vertical setup. The basis of the measurement methods were tested in static environments. Afterwards a horizontal and dynamic setup is described more in detail. In the following sections, topics are not in chronological order, but in a natural order for the overall development of method.

3.1 Vertical Pipe Setup

The purpose of this setup is to measure the temperature of a fluid at two places in a known distance and calculate the difference in time in which the thermal pulse reaches the two sensors. This is a feasibility study to determine whether the fast response temperature probes from Pasco and a light bulb can function for registration of thermal pulses in fluid.

3.1.1 Vertical Experimental Setup

Before the analysis, a construction was built consisting of a transparent acrylic pipe placed vertically onto a plate made of PVC. Figure 3.1 illustrates the vertical pipe setup.

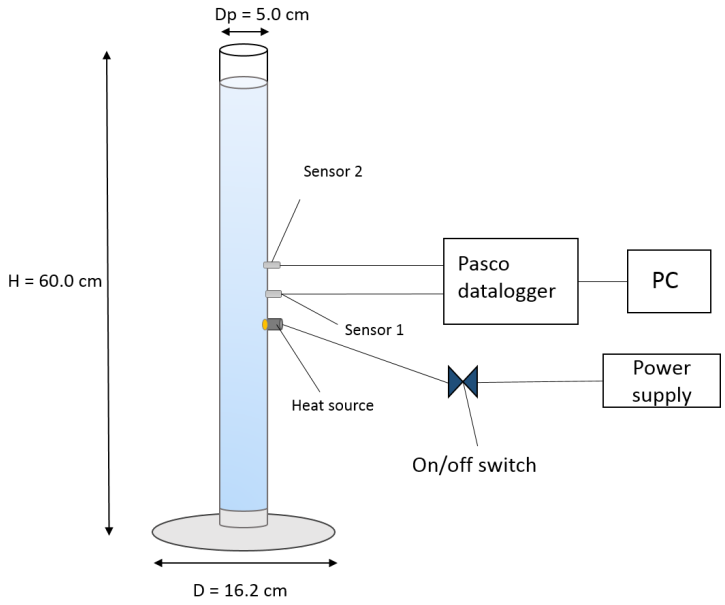

Figure 3.1: Illustration of the vertical pipe setup

The one end of the pipe placed onto the plate was completely sealed using silicon. The construction had the following measurements: height 60 cm, inner diameter of pipe 4.0 cm and wall thickness of the pipe 0.5 cm. Two temperature probes and a light bulb used as heat source were positioned in a vertical order 30 cm up the pipe. The two temperature probes were placed with a separating distance of 1.0 cm. By placing probe 2 straight above probe 1 the distance from the lower probe to the heating source were 2.0 cm. All components were placed in line with the pipe wall by drilling holes into the pipe and using silicon to attach them.

Equipment from Pasco were used for measuring temperature. The temperature probes used were the PASPORT Fast Response Temperature Probes PS-2135, these were each connected to a PASPORT Absolute Pressure/Temperature Sensor PS –2146 and the PASCO® 850 Universal Interface. The program PASCO Capstone was used to record data from the sensors. A halogen light bulb (20 W,

12 V) represented the heat source in this setup, it was connected to a Manson SPS-9602 switching mode power supply. Between the light bulb and the power supply, a light switch were mounted in order to apply heat pulses into the fluid. Specifications of the instruments is in Appendix A.

3.1.2 Vertical Experimental Method

To be able to measure the time shift of a heat pulse between the two temperature probes, the pipe was filled with distilled water. The experiments were performed by applying heat pulses into the fluid. Heat pulses was sent by turning on the light bulb for a couple of seconds and of again, such that heat from the light bulb was applied to the fluid. The two temperature sensors measured the temperature of the fluid continuously. Several heat pulses were applied into the fluid to examine how the change in temperature was registered. Temperature data from the two sensors was recorded and analysed.

3.1.3 Analysis and Observations

In this static experiment, the purpose was to find out if the setup of the temperature probes and heat source gave a definable registration of heat pulses through still water.

Observations of the temperature data showed that the sensor further apart from the heat source followed the same pattern of heat pulse registration as the sensor closest to the heat source, but it seemed to have a more rounded change in temperature measurement. The closest sensor registered every little change of temperature in a more irregular pattern. It was likely to believe that the heat diffused in the fluid and as the distance from the heat source increased, impact of the heat decreased. It was difficult to see a noticeable time shift between the two peaks in temperature measured by sensors.

Comparison of the temperature data from the two sensors resulted in a linear relation between them with a regression coefficient R^2 equal to 0.9423. Which implied a good registration of heat pulses in still fluid. The light bulb placed at

the pipe wall did function as heat source in this experiment.

The probes and heat source was placed in the middle of the pipe. This way, the water column was sufficiently high above the probes to ensure that the heat flow in the water behaved in an approximately natural way, and was not disturbed by change of direction when reaching the water surface.

The Pasco equipment seemed adequate for temperature registrations, the temperature probes measured instantaneously changes of temperatures with a high resolution. Specifications of the temperature probes are [21]:
Range -30 to 105 degrees Celsius
Accuracy +- 0.5 degrees Celsius
Resolution 0.01 degrees Celsius or better.

Based on these results, it was desirable to continue the development of the measurement method for low velocities using measurement equipment from Pasco.

3.2 Horizontal Pipe Setup

The vertical pipe setup showed that the concept of using Pasco temperature sensors and a heating source did function for measuring instant heat pulses in fluid. Therefore it was desirable to take the concept further and check the conditions in a system with fluid flow. The following experiment was performed to determine whether it was possible to measure the velocity of fluid flowing through a horizontal pipe system.

3.2.1 Horizontal Experimental Setup

An experimental construction was built in advance of the experiments. A schematic drawing of the horizontal pipe setup can be seen in figure 3.2.

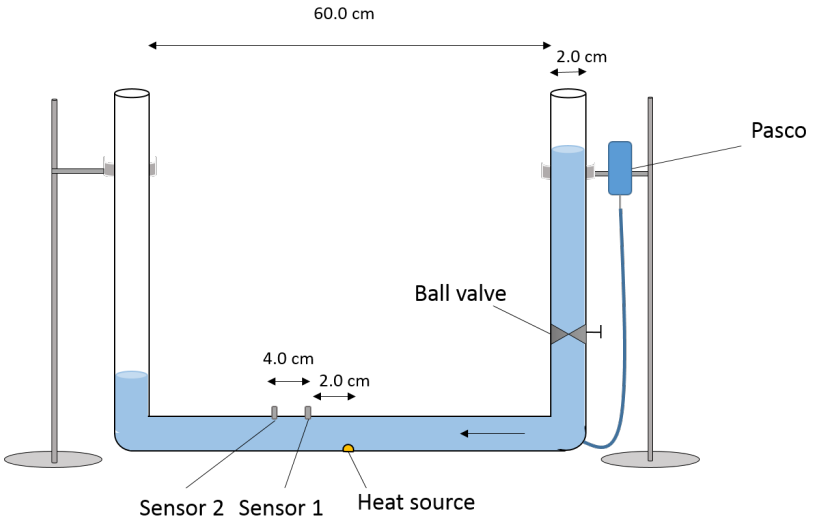

Figure 3.2: Illustration of the horizontal pipe setup

The horizontal setup was made of pipes connected in an u-shaped construction, held up by two tripods. The construction consisted of three pipes made of transparent acrylic with an inner diameter of 2.0 cm and outer diameter of 3.0 cm. One of the pipes was placed horizontally, it was connected to the two other pipes by acrylic bend on both ends. The pipes and bends were connected so that there was no leaks out of the system when it was filled with fluid. At the middle of the horizontal pipe, a heat source and two temperature probes were attached to the pipe wall by drilling holes and using silicon. The distance between the temperature probes were 4.0 cm, and between the first probe to the heat source 2.0 cm. In this setup the heat source was positioned on the opposite pipe wall relative to the temperature probes. On the right vertical pipe a ball valve was installed. On both of the two vertical pipes, a metric scale was attached, for easier measurements of the water level in the pipes. Equipment for collecting measurement data and the voltage source used was the same as in the vertical pipe setup. The setup was modified and optimized several times since new solutions were developed after working with the setup.

Modifications and Optimization of Experimental Setup

The optimization was a process followed by a lot of trail and error until a result that satisfied the needs and criteria for this experimental setup and method was reached.

As the ball valve did not appear as the most accurate measure of inflow, a modification was to attach a protractor onto the handle of the valve. An image of this is shown in figure 3.3. The protractor was used as a measure of valve opening. The valve was totally closed when the protractor was positioned vertically at 0 degrees, and as the valve was opened, the number of degrees increased. In the experiments performed, the valve openings used were between 5 and 10 degrees. To gain a better understanding of what inflow a 5 degree opening of the valve represented in units of cm^3/s, a study of the variation in inflow rate and average flow rate of different degrees was carried out.

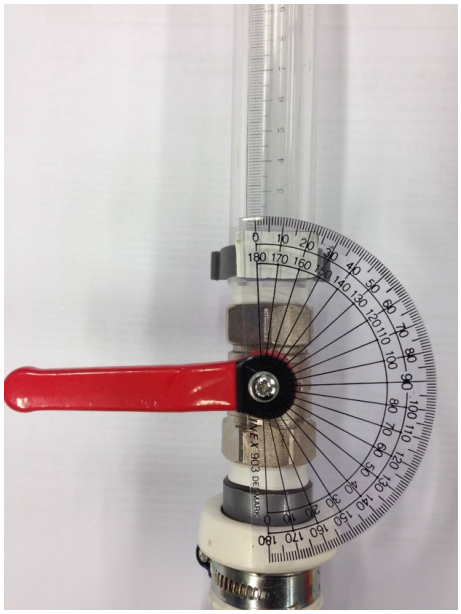

Figure 3.3: Image of the protractor mounted to the ball valve handle

To control the measurement technique a pressure sensor was added to the system. Pasco PASPORT Absolute Pressure/Temperature Sensor was used. The condition for using this equipment was that the sensor should not be in directly contact with the fluid. The solution was to install a flexible tube in the bend on the same side as the valve, and connect it to the sensor. An illustration of the setup for the Pasco equipment is shown in figure 3.2. The tube was filled with fluid up to a certain level H_l. Above this level the tube was filled with air, see figure 3.4.

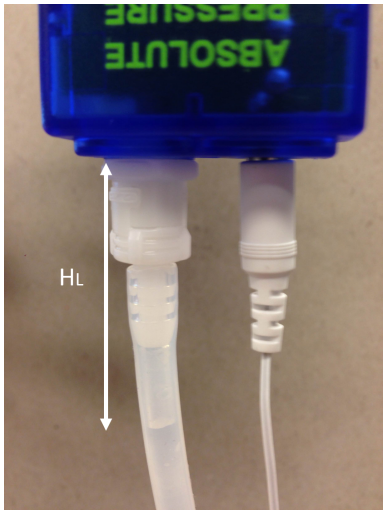

Figure 3.4: Image showing height of air,H_l in tube connected to sensor

The sensor measured the pressure of the air as an indication of the pressure in the system. As fluid flew through the system, the fluid was pushed into the tube so that the fluid level in the tube rised and pressurized the air. Thus the measured pressure increased. Gradually as the flow rate started to decrease, the rate of increase of pressure declined as well. When the equilibrium level of the vertical pipes was reached and the flow stopped, the measured pressure became approximate constant.

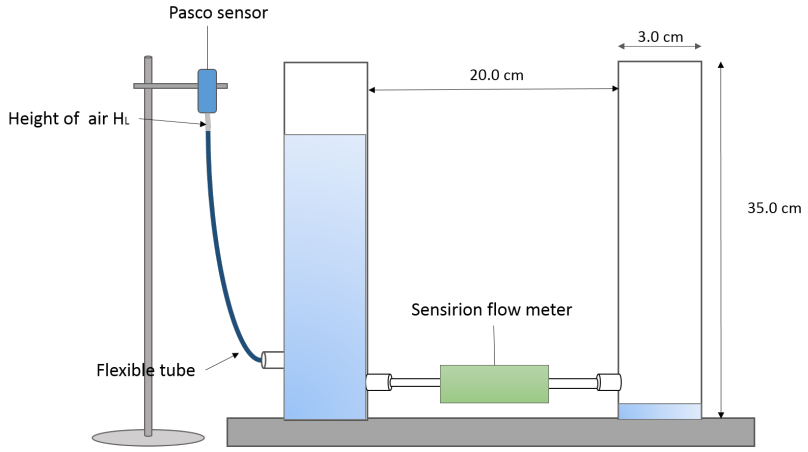

Figure 3.5: Illustration of setup for calibrating pressure measurements performed by using Pasco equipment and Sensirion flow meter

Afterwards it was decided to perform a calibration of the pressure measurements. A setup for calibrating the pressure measurements from Pasco Absolute Pressure/Temperature Sensor was made, illustration of this setup is given in figure 3.5.

The setup was built using pipes of the same size as in the horizontal setup. A SLS-1500 liquid flow meter from Sensirion was applied, specifications is given in Appendix A. The resulting pressure and flow rate measurements were analyzed to determine the relation between flow rate measured by the Sensirion flow meter and the indirectly flow rate calculated from pressure data measured using Pasco equipment.

Based on the first measurements, the temperature probe placement needed a significant optimization. At first, the purpose was to place the temperature probes and heat source in line with the pipe wall, to inhibit as much disturbances of the flow as possible. However, because of the high sensitivity of the temperature probes, the temperature from the surroundings were measured as well as the temperature of the fluid. To eliminate the effect of temperature of the surroundings, the temperature probes were placed in a way that the whole probe was inside the pipe and in direct contact with the fluid. In this case the two sensors were not placed inline with each other, because one would eliminate the possibility of one sensor lying behind the other one which would give an uneven heat distribution. It was experienced that the wire connected to the probe conducted heat from the surroundings. Tests to examine the influence on the total temperature measurements were therefore performed. The results showed that the probe registered heat up to 10 cm from the tip of the probe. It was therefore decided that the final placement of the temperature probes was to also include the first 10 centimetres of wire from the probe tip in the pipe, see figure in Appendix D. This way the temperature of the surroundings had a minimum effect on the temperature measurements in the fluid. The temperature probes and the following wires were attached horizontally on to the pipe wall, with the tip of the probe facing downwards into the center of the pipe.

Based on the result of the vertical case, the first heat source used in this setup was a halogen light bulb with the specifications: 7 W, 12 V. More concentrated heat distribution was considered to give a more resolvable measurement of heat pulses, flow rate. All this time using a light bulb was considered to give a wide heat distribution into the fluid since the heat was likely spread into the fluid from

the entire geometry of the light bulb.

Other alternatives to heat sources were studied. However, the fact that it should tolerate both fresh water and salt water made it more complicated. This was among the reasons for finally deciding to use a light bulb with higher power as heat source in the following experiments. The light bulb used in the final setup was a halogen light bulb of 50W and 12V.

First the heat source was placed as in the vertical setup, in line with the pipe wall. But as the placement of heat source had also been of interest in relation to flow pattern and distribution of heat in the pipe, it was decided to move the heat source further into the flow.

Another idea was to measure the amount of voltage sent through the light bulb, while the heat pulses were applied. A Pasco Voltage Current Sensor was connected to the wires of the light bulb, specifications of the sensor is in Appendix A. From these measurements an exact measure of the duration of the heat pulses could be achieved.

A additional study on the dynamics of the heat pattern was performed using PIV. The principles of PIV is explained in section 2.6. This analysis was performed in a new setup where a visual analysis of static and dynamic cases were performed. Figure 3.6 illustrates the setup made for this analysis. This setup gave a better insight of the heat pattern in fluid.

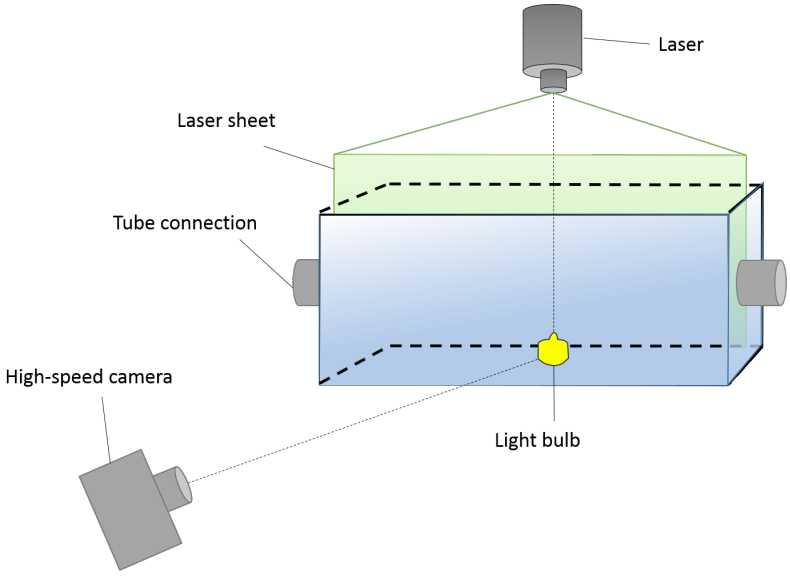

Figure 3.6: Illustration of setup for visualizing heat distribution from the heat source into the fluid

3.2.2 Horizontal Experimental Method

During the development of method using the horizontal pipe setup several new aspects were discovered. To this end a closer look at the experimental methods described below are not only the main technique but also methods of the preliminary studies of the technique. The working fluid used in the following experiments was distilled water.

Measurement of very low flow velocities

The horizontal setup was filled with distilled water and the valve fully opened to avoid air bubbles. Prior to the experiments the valve was closed, and the left pipe was emptied for fluid down to the bend by using a syringe. The right pipe was totally filled with fluid, see figure 3.2. The heat source was then connected to the power source and to the voltmeter. The tube, which measures pressure was filled with fluid. The air level,H_l, were set equal to 4.5 cm from fluid level in tube to the sensor including the connection to the sensor, see figure 3.4. Temperature probes and pressure tube were connected to the Absolute Pressure/Temperature Sensor. The voltage used for the heat pulses was set to a particular voltage. After setting up the equipment, the software on the computer was ready for data acquisition.

This was the procedure adapted in every experiments. The valve was then opened to a certain degree of ball valve opening: 5^{o}, 7^{o} and 10 ^{o}. Heat pulses was applied to the fluid by switching the light bulb on for a few seconds then of. A couple of heat pulses was applied into the fluid during flow. In general the flow rate will decrease as the liquid level is decreasing. When the equilibrium level was reached the recording of measurement data was stopped. These procedures were performed for different flow rates and voltages. After collecting measurement data, a processing and analysis was done.

The data was analysed using the cross-correlation function in order to find the time shift between the temperature peaks of the heat pulse measured by the two sensors. The time shift, Δt, was calculated using a MATLAB program $Flow\_ccf\_june_{R}WT.m$. By comparing the data measured by the two sensors and finding the time shift between them, the average velocity of flow could be calculated.

Prior to the described experiments preliminary test in order to have a definable time shift was done. Measurements were carried out for different voltages and flow rates. The voltage varied from 6 - 10V. The purpose was to measure for which conditions it was possible to find time shift of heat pulses for this experimental case. Determining the optimal flow rate and voltage power necessary to have a definable registration of time shifts between the two temperature sensors. To be able to calculate a time shift, a definable heat peak has to be present in the measurement data. Experiments were repeated several times and data was collected with a sampling rate of 20 Hz.

Inflow measurement

A study of rate of inflow was performed for the rates of 5^{o}, 7^{o} and 10 ^{o} ball valve openings. The horizontal setup was filled with fluid in the same way as for the measurement of flow velocities. The measurements were performed without applying heat pulses into the fluid. The fluid flow through the system with the rates of 5^{o}, 7^{o} and 10 ^{o} ball valve openings, while the pressure was measured.

In addition, the duration of the decrease in water level above the ball valve was measured. The duration of flowing each centimetre of water height was measured. The flow rate measurement for the ball valve was repeated several times to get an estimate of possible errors. The average volumetric flow rates of the different valve openings were then calculated.

Pressure calibration

The pressure measurement validation was accomplished by calibration between the pressure measured by Pasco equipment and measurements from the Sensirion flow meter. The relation between them will be used throughout the experiments. The calibration of pressure measurement from Pasco Absolute Pressure/Temperature Sensor were performed using the setup in figure 3.5. A flow meter were used in this setup to measure the flow rate. The flow meter was a Sensirion SLS-1500 which is a highly accurate flow meter and can measure up to 40 ml/min, specifications in Appendix A. It was placed between the two pipes and was connected to a tube in which the fluid flew through between the two pipes. The sensor from Pasco was connected by a tube to the pipe in a connection placed higher than the one for the Sensirion flow meter to avoid dynamic pressure. Before running the experiments the pipe on the same side as the Pasco sensor was filled with water. When the experiment started, both the Pasco sensor and Sensirion sensor recorded measurement data. The flow rate and pressure were measured until the equilibrium of fluid level for the two pipes was reached.

Experimental data was analysed using MATLAB and MS Excel. Due to the high sampling rate of the pressure data, averaging of the measured pressure and time was needed and performed in MS Excel. The averaging method was made in every twentieth points to minimize the amount of data to analyse according to equation 2.7 in section 2.5.2. The time series from the Sensirion flow meter were of an uneven time series. To be able to compare it with the measured pressure, a program $Marta_averaging_1.m$ in MATLAB was used, see Appendix B. This program created a new and even time series by interpolating 'nearest' the measured velocities. The data sets were compared by a unity-based normalization

of 187 data points. The results will be given in chapter 4.

Determination of the heat source

In order to test the measurement technique a heat source that would apply a more concentrated and direct heat pulses into the fluid was needed. Initially a light bulb as used in the vertical case was used for the horizontal case, see section 3.1.1. But visually the surface of the light bulb created a wide distribution of heat. Therefore studies of other heat sources were performed.

One option that was considered as potential was to create a heating element using tungsten wire. Tungsten wire has suitable characteristics to be used as a filament. Tungsten has a high melting point, high resistant to corrosion and conducts heat effectively, which would be suitable for sending concentrated heat pulses into fluid [22]. However, constructing a filament of tungsten was complicated since the Tungsten wire, D=25 μ meter, is difficult to weld and our requirement that the filament and its connection should tolerate water. This option was then omitted since this will be time-consuming.

Another option was to use the existing filament of a light bulb. By doing so one could avoid the difficulties of constructing a heat element and easily use the already installed connection of the light bulb. This idea was tested by breaking the glass covering the filament of a 5W, 12V light bulb. The resistivity of the remaining bulb was tested with a multimeter to check if the filament was complete before continuing testing this option. The light bulb was connected to a voltage source and the part of the light bulb with the filament was immersed into a vessel filled with distilled water. Figure 3.7 illustrates how the filament was entirely surrounded by the fluid.

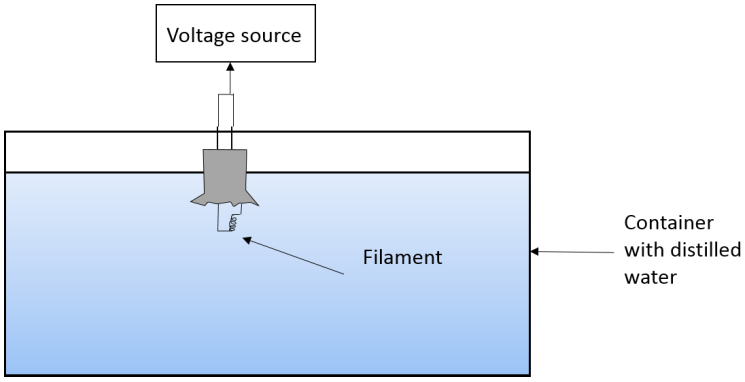

Figure 3.7: Illustration of test setup of light bulb filament

When the filament was placed under water, voltage signal was sent through the filament. As voltage power was increased the filament quickly became overheated and for a voltage of less than 5 volts the filament was torn. Uncertainties concerning whether the heat applied from the filament would be sufficient as a heat pulse in the pipe was among the reasons not choosing this principle as a heat source.

Important criteria for selecting heat source was its ability to withstand direct contact to the fluid. The final choice of heat source for this experimental setup was to change the light bulb into a powerful, 50 W, even though this did not improve the distribution and concentration of heat pulses.

Visualization of heat pulse

Initially an analysis was performed in the horizontal pipe setup, by illuminating the pipe where the light bulb was placed. When a heat pulse was sent into the fluid, it was visible how the heated fluid travelled from the surface of the light bulb and through the adjacent fluid. The density changes due to temperature differences was then considered to be the only driving force in buoyant flow like this. Seeding particles were added to the fluid in order to improve the visualization of the heat rise. By adding seeding particles into the fluid, it was possible to visualize the dynamics of the fluid indirectly by illuminating the seeding particles. The movement of the seeding particles in the horisontal pipe setup were recorded using an Iphone 6 (240 fps).

To gain a better understanding of how the heat distribution from the applied heat pulse was, the setup illustrated in figure 3.6 was made. To begin with the setup consisted of a cylindrical container, but due to optical disturbances a rectangular container was chosen. The setup consisted of a rectangular transparent container(6.6x6.6x10.0 cm) where a light bulb was placed in the center from the bottom. The light bulb was mounted in a drilled hole and placed halfway into the container. On two of the opposite walls of the container connections for a tube was placed in the center, as shown in figure 3.6. The connections were closed in the beginning, but later a tube was connected so to make flow through the container possible. The container was filled with fluid injected with seeding particles.

The technique used to visualize the distribution of the heat emitted from the heat source was particle image velocimetry(PIV). Copolyamid particles were used as seeding particles and was added to the fluid. The fluid was illuminated by a DPGL-2200L laser, which is a continous laser with a wavelength of 532 nm and an output power of 200 mW. The laser illuminated the container with a light sheet placed straight across the heat source, the thickness of the light sheet was 1.5-3 mm. The high-speed recording camera was a Basler acA800-510uc USB 3.0 camera, specifications in Appendix A. A rate of 200 fps was considered sufficient to capture the dynamics of the flow.

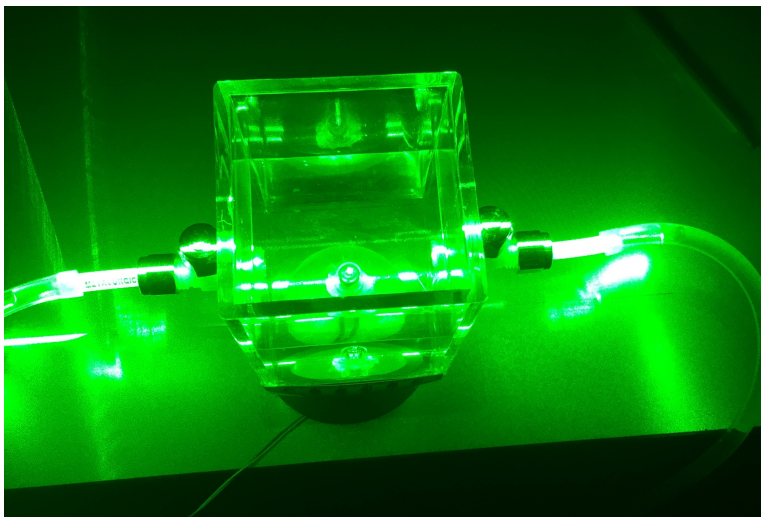

Figure 3.8: Image of container illuminated by laser sheet in the analyse of heat visualization, view from the top.

Figure 3.6 and figure 3.8 shows an illustration of the setup where the container is illuminated by laser across the light bulb and a top view picture showing the placement of the laser sheet respectively. The fluid pattern was recorded while heat pulses were applied, both with and without external flow in the container. The videos were later processed and analysed using PIVlab version 1.4 in MATLAB. PIVlab is a time-resolved digital PIV tool for MATLAB [23].

Static experiments with no flow across the container except flow from the heat pulse were first performed. The power of the heat source was 7.35 W. The recording of fluid movement was started before trigging the heat pulse and continued a while after the heat pulse was stopped.

For the dynamic experiments with flow across the container, a pump was installed to the tubes connected to the walls of the container. The pump was an inline pump of 12 V used to circulate the fluid through the container. A Manson SPS-9602 switching mode power supply was used with the pump. The rate of the pump was controlled by varying the voltage, so a calibration of pump rate were performed to be able to measure rate in cm^3/s. The calibration was performed using a Sensirion SLQ-QT500 flow meter, specifications given in Appendix A. The flow rate was measured from a voltage of 2.0 down to 0.7 and up to 2.0 to find the flow rate in cm^3/s. This was done to see any hysteresis from the pump. The data from the calibration of pump was first processed to have an even time series by interpolation with the nearest values in the data. Then, the average of the interpolated data were calculated. The result was a linear expression of the pump rate, and a hysteresis was observed as seen in figure in Appendix C.

Recording of movement of the particles was started before the fluid was flowing. Then the pump was started with a flow rate of 0.35 cm^3/s. The pattern of the initial flow into the container was recorded and looked into. As the flow became more steady through the container a heat pulse with the power of 7.35 W was applied for 4 seconds. It was observed that the inflow and heat jet did not reach entirely through the container. Therefore, the flow rate was increased to 1.50

cm^3/s. With the higher flow rate a new heat pulse was applied to the fluid, the recording was stopped 3.5 seconds after the last pulse.

Prior to using PIVlab, several MATLAB programs were used in processing of the experimental data. In the earliest experiments with PIV, an Iphone 6 was used to record a video of the fluid movement. This movie had to be splitted into single frames, before performing PIVlab analyse. A MATLAB program, vdosplit, was used for splitting the video into single frames, see Appendix B. For the experiments recorded with the Basler camera, the output was bitmap image format. Both of these cameras recorded in RGB, so to be able to gain a better resolution and analyse in PIVlab, the frames was converted from RGB into grayscale. A MATLAB program called conv_gray was made to do this conversion, see Appendix B.

A selection of image frames were uploaded in PIVlab to be analysed. Before performing the analyse a preprocessing had to be done. Region of interest was set equal to the inside of the container. To gain a better resolution and contrast in the frames different filters were applied to the frames. Filter used varied for the different recordings according to the quality of the images. Among the analyse settings were CLAHE, enable intensity capping and PIV settings: analysis of 3 passes used. CLAHE stands for Contrast-limited adaptive histogram equalization, which is a filter that locally enhances the contrast in the images. Intensity capping is used to set an upper limit of the greyscale intensity to avoid that brighter particles contributes statistically more to the correlation signal. PIV settings is set to determine the setup of the cross-correlation of image data. The passes is used to determine the interrogation area and to choose vector resolution, that is vectors per frame [23]. Analyse of all image pairs was performed. A post-processing of the results was to do a vector validation, where erroneous vectors were removed and interpolated by setting velocity limits. The calculated vectors had the unit of pixels per frame. Conversion into meter per second was performed by a calibration. A calibration image was used to set a known distance and the time step Δt was set according to the sampling rate used recording the video. The next step in

processing was to modify the plot appearance. When this was done, different parameters was easily extracted in PIVlab.

Results and Discussion

Development of this method has involved a wide spectre of ideas and possibilities. A horizontal pipe setup has been the basis of developing the method, and from working with this setup several ideas and necessary tests have been performed to improve and test the method using this setup.

4.1 Measurements of Very Low Flow Velocities

As mentioned earlier the cross correlation function technique was chosen to be a good candidate to analyse the temperature data from the two sensors in the horizontal pipe setup. A problem with the method in relation to this experimental study was that the sensors registered the heat pulse in approximately the exact same moment. There was not a definable time shift between the registrations for several flow rates and heat pulses.

An experiment conducted in the vertical pipe setup where a time shift appeared is given as an example of the cross correlation analysis in MATLAB. The results of the analysis is given in figure 4.1 and 4.2. The data series was recorded with a sampling rate of 50 Hz, the data shows the recording of one applied heat pulse.

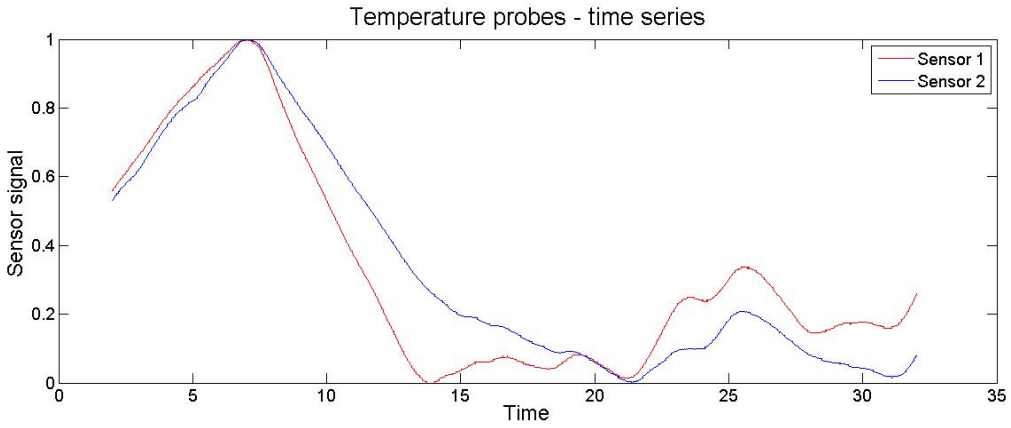

Figure 4.1: Comparison of normalized data

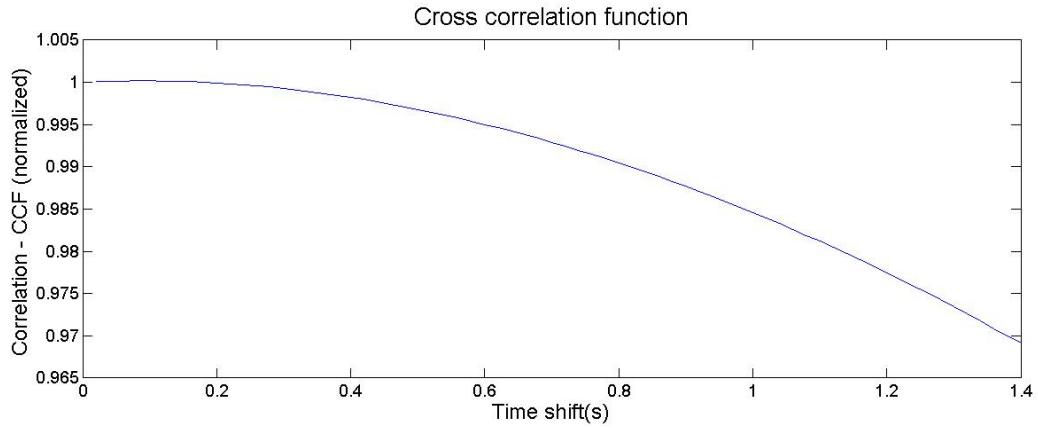

Figure 4.2: Comparison of normalized data

The temperature data from two sensors are normalized and plotted as time series in figure 4.1. Temperature registered by sensor 1 is given in red, while temperature registered by sensor 2 is in blue. The results of a cross correlation of the normalized data is given in figure 4.2. From this plot a maximum calculated time shift is 4 time steps which equals a duration of 0.08 seconds. That is, it takes 0.08 seconds from heat is detected by the first sensor until it is detected by the second sensor. With a distance of 1.0 cm between the probes the average velocity of the thermal pulse would be 8 m/s which seems to be high. The registration of signals is decisive in calculating average velocity. In this example the two sensors detects the signal in approximately the same moment. This indicates that the signal is scattered into the fluid with random boundaries and does likely not maintain a constant shape. This gives reason not to use the cross correlation function

uncritical, but be aware that the physics of the signal and its surroundings is crucial for the transmission of the signal.

However, since the experimental setup did not register clear heat peaks it was difficult to perform the analysis with cross correlation. The problem with registering clear heat pulses could possibly be due to geometry or the measurement equipment used. Disturbances of flow pattern could result in indistinct heat pulses.

An alternatively better method to provide the heat peaks is to make sure that the flow is one dimensional in pipes of smaller diameter. In one-dimensional flow the effects of fluctuations of the flow are limited as well as heat diffusion.

As the idea of performing cross-correlation analysis to calculate the velocities did not work out the way it was desired, a simplified method had to be used. As the pressure in the system was measured through each experiment and the pressure measurements was calibrated using the Sensirion flow meter, the relation between flow rate and pressure measurements could be used as an indication of the velocities in the system. This will be explained in the following section.

4.2 Pressure Measurement

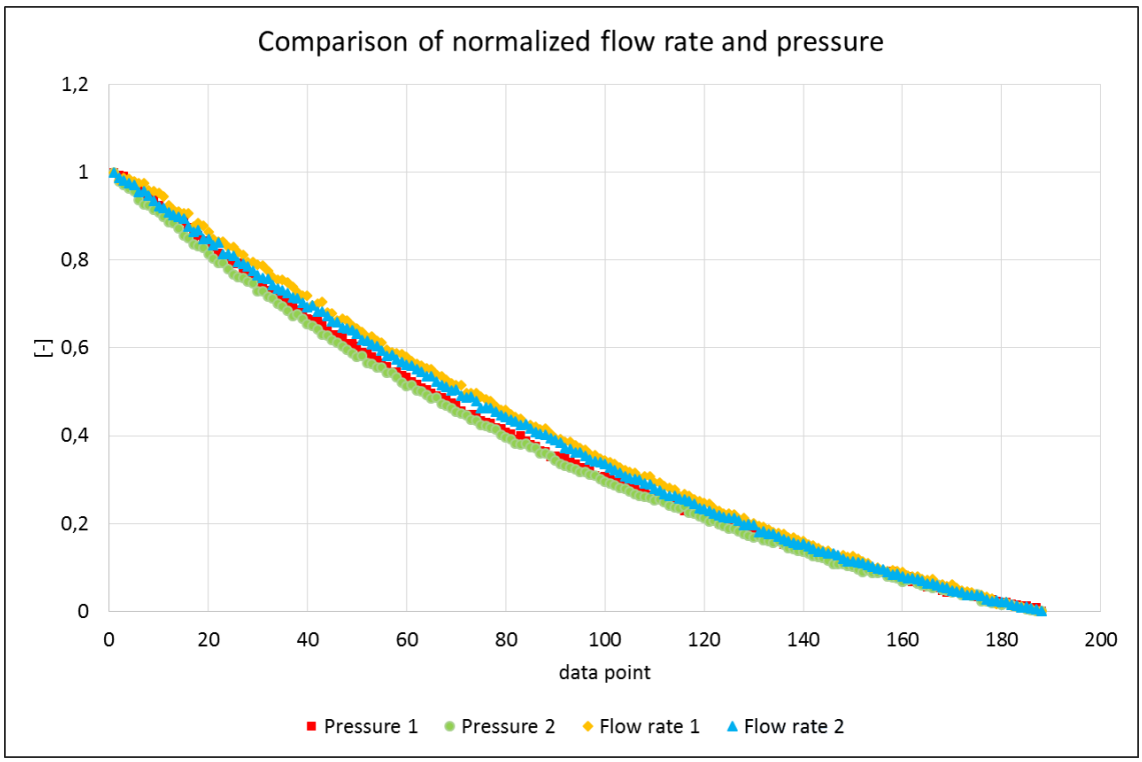

Figure 4.3: Data comparison of normalized flow rate and pressure

Results of the pressure calibration are given in figure 4.3. The plot shows a comparison of normalized data sets of pressure measurements from Pasco sensor and corresponding flow rate from Sensirion flow meter. In the plot the results of two experimental runs, 1 and 2, are given for comparison. The pressure measurements show a similar trend compared with the flow rate. The pressure curves are slightly lower in some areas compared to the flow rate, this is shown in both cases.

Due to the fact that the Pasco pressure sensor could not be directly in contact with the fluid, an alternative method for measuring the pressure had to be considered. The choice was to measure the pressure of the air level in the tube as an indication of the fluid pressure in the pipe system. In this case it is assumed that the air compressibility is neglected.

The sensitivity of the pressure measurements are height of air in tube H_l (see

figure 3.4) and disturbances from the surroundings. The smaller the air bubble, the better resolution of the pressure measurements. Pressure measurements were highly sensitive to noise from the surroundings and recorded it. E.g. when a person came into the room the vibrations of the steps were instantly recorded and was seen from the pressure leaped outside its 'normal' trend. Figure 4.4 is a cropped image of the Capstone program where the noise in the pressure measurements is encircled. In this figure, measured pressure (kPa) is given as time series (s).

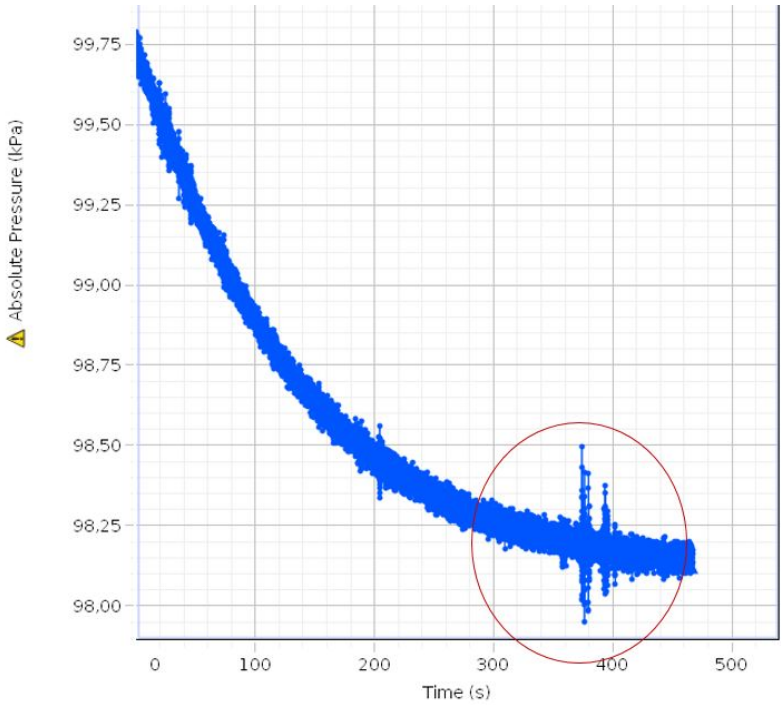

Figure 4.4: Extracted image from Captone showing pressure measurements with noise encircled.

4.3 Inflow Control

In this experimental construction a ball valve was seen as adequate for controlling the flow through the system. However, the ball valve is a source of uncertainty. The valve has a rough opening system in which the characteristics of the 'ball' affects the amount of fluid flowing through the valve. This is seen in the results from the study of the average flow rates of different degrees valve opening and the variation in inflow rate.

The study of inflow using ball valve openings of different degrees is based on experiments conducted 10 times for 5 and 10 degrees and 14 times for 7 degrees. The initial water column height in the pipe was 16 cm the fluid was drained to a level of 6 cm. The results with corresponding standard deviations of these experiments are shown in figure 4.5 and in table 4.1.

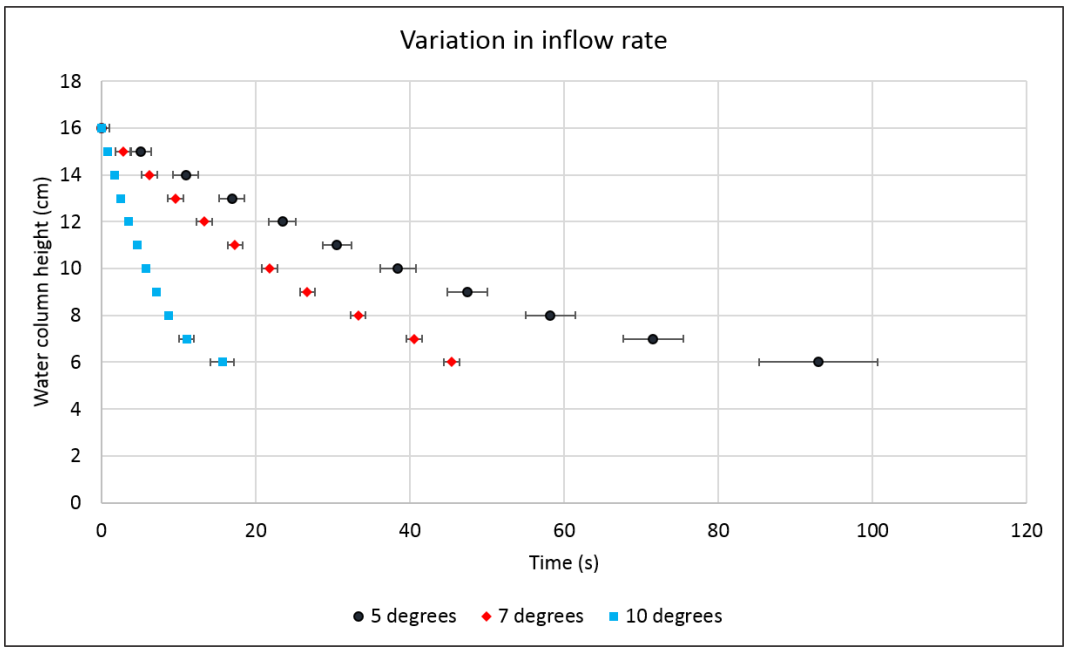

Figure 4.5: Flow rates of different valve openings with corresponding standard deviation

Figure 4.5 shows a plot of the measured average duration of decrease in water column height as a time series for different valve openings. The corresponding standard deviation is shown for each level of water column height, by a vertical marker. The experimental data shows an increasing trend for the duration of flowing one centimetre of water. From these results it can be clearly seen that the deviation increases as the rate of inflow decreases. Largest deviation is found in data for the 5 degree valve opening, where the deviation is increasing steadily as the water level lowers. For the two other valve openings the deviation is smaller. An equivalent exponential trend is shown for the pressure data recorded simultaneously. The change in pressure increased significantly when the water started to flow and gradually declined as the rate of inflow was lowered. As the

inflow stopped, the pressure measured was approximately constant.

Table 4.1: Calculated average volumetric flow rates with corresponding standard deviation

Degrees	Average flow rate (cm^3/s)	Standard deviation σ	Standard deviation as % of average flow rate
5	0.37	0.10	27
7	0.64	0.12	19
10	2.12	0.13	6

In table 4.1 the calculated average volumetric flow rates in units of cm^3/s with standard deviation are given. The standard deviation is also given as percentage of the average flow rate. The calculated values clearly shows how the volume of inflow is changed by changing the degrees of valve opening. In accordance with the results in figure 4.5 the calculated values shows that the deviation is largest for the opening of 5 degrees. The valve opening which has the lowest deviation of inflow rate of the three valve openings, is the 10 degrees valve opening. From these results it is clearly shown ow the volume of inflow changes with respect to degrees of valve opening.

An aspect of using a ball valve for controlling inflow is the ball valve characteristic. The characteristic of a ball valve is a subject of interest in relation to the accuracy of inflow rate. As mentioned in section 2.7, the ball valve has poor throttling characteristics which can result in poor accuracy of inflow rate. Another effect of throttling is the increased possibility of cavitation. Throttling may lead to regions of local low pressure in the valve which can cause cavitation.

An optimal rate of inflow in relation to heat pulses is necessary in order to test the concept of the measurement method using the horisontal setup. To be able to have a clear registration of heat pulses, a certain rate of inflow has to be used. If the rate is too low, the heat pulse will probably diffuse before reaching the second sensor. If the rate is too fast, it will be difficult to distinguish the temperature sensor registrations of the heat pulse. Thus, the optimal rate of inflow is when there is a clear difference in time of the registration from the two sensors, so that it is possible to find an exact time shift.

4.4 Heat Pulse

During an experimental run fluid flow through the pipe and heat pulses is applied from a heat source. Choosing the heat source to be used testing this method, is an important item of discussion. Several experimental runs were made to find the optimal source of sending concentrated heat pulses into the fluid.

4.4.1 Heat Source

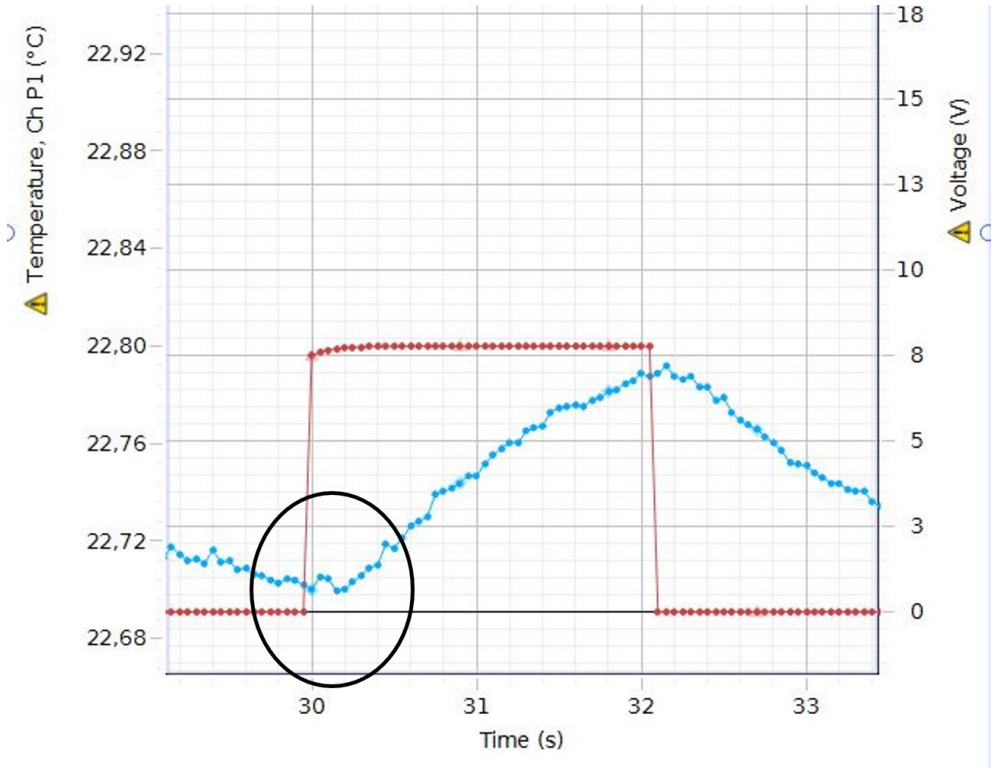

Figure 4.6: Plot extracted from Capstone showing voltage versus temperature of sensor 1 during a heat pulse. Time lag is encircled.

The filament of a light bulb is covered by gas and glass, which can possibly cause a time lag of the heat pulse even before it reaches the fluid. Specific tests concerning time lag was not conducted. However, looking at the voltage and temperature measurements from sensor 1 one can see an indication of a lag. Figure 4.6 shows a subplot extracted from Capstone from an experiment conducted with the 50W light bulb used as heat source. This subplot is of a measured temperature and

voltage at moment a heat pulse is applied into the fluid. As seen from this plot, the voltage is a rectangular pulse while the measured temperature gradually increases as long as voltage is sent through the light bulb. Encircled is the time in which the voltage is turned on and the change in temperature due to this. The time between the voltage is turned on and a registered change in temperature of fluid is less than 0.4 seconds. In the duration of 0.4 seconds power is sent through the filament in the light bulb and all the way through the fluid before reaching sensor 1. Probably, if there exists a time lag using the light bulb it is significantly small.

The placement of the light bulb was also under discussion in relation to applying a definable heat pulse. Whether the light bulb should be placed in in line with the pipe or in center of it. Figure 4.7 shows illustrations of possible patterns of the heat pulse relative to position of heat source. If the light bulb was placed close to the pipe wall, it is possible that the heat pulse will bend across the whole cross section of the pipe and be distributed as a cloud of heat. The area of lower velocities close to the wall could affect the distribution of heat pulse. On the other hand, if it was placed in the center of the pipe and directly in the area of the fully developed velocity pattern, one could imagine that the heat pulse would follow the velocity profile of the flow.

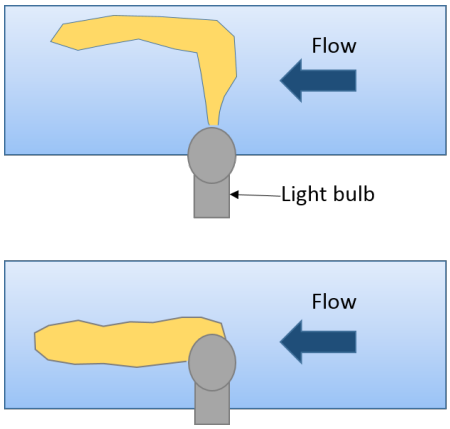

Figure 4.7: Figures showing possible heat flow due to different placements of heat source in pipe

An aspect to be considered concerning this measurement method is that the flow meter itself carries out a heat transfer. The light bulb chosen as a heat source in this experimental setup conducts heat to the surrounding pipe walls and air

as well as to the fluid. The pipe walls are quickly heated as the heat pulse is applied.

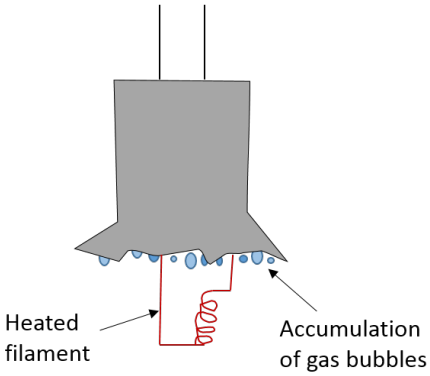

Figure 4.8: Illustration of filament of light bulb

The idea of using a filament of a light bulb resulted in a torned filament. When the glass surronding the filament was broken, some of the glass was left to ensure not to break the filament. One may assume that the restoring glass covering the filament lead to an accumulation of gas at the end of the filament, see figure 4.8. Another possibility is that a film of gas covered the filament as power was sent through the filament and heated it. Whether the filament was covered by a gas film or gas was accumulated, it is possible that it is not be enough coolant present to avoid overheating of the filament. Both of these proposals could result in overheating due to lack of cooling, and was therefore not seen as a potential heat source in relation to this experimental setup.

A possibility in further study of this method is to develop a heat source using tungsten wire or similar. Where the surface area of the heat source is smaller and placed in the optimal position of the pipe in order to send out distinct heat pulses which can easily be registered. A benefit of using tungsten is its high resistance of corrosion. So it would be suitable to use in relation to the NORTH loop where the fluid has varying salinity.

4.4.2 Application of Heat Pulse

The voltage of the heat source was measured by a voltmeter and controlled by a light switch as a heat pulse generator. In these measurements it was made possible

to know the exact duration and start/stop time for the heat pulse. Figure 4.6 shows an example of such a heat pulse. Uncertainties related to possible time lag from using a light switch is neglected. The Pasco voltmeter measuring voltage of the light bulb is registering pulses as step deterministic signals, and the voltage measured by Pasco voltmeter deviates with $\pm$ 2.5 % compared to what the voltage source is set to.

A possible problem that appeared concerning the light bulb used as heat source is overheating. When the light bulb is on, the water surrounding it starts to boil. This happened both in the horizontal pipe setup and in the setup for testing the heat distribution from the light bulb. This is a limitation to the heat source used in the experiments, the light bulb heats up the surrounding fluid but also the material surrounding it. In this case the acrylic pipe clearly becomes warmer when heat pulses is applied. Voltage power and duration of heat pulses should be set in order to minimize the possibility of overheating.

Impact of Heat Pulse

The amount of energy that is needed to be applied into the fluid to get a quantifiable temperature change can be calculated. The following is a simplified example of impact in an applied heat pulse in still water.

A heat element is placed in a circular pipe with an inner diameter of 2.0 cm. We assume that the fluid is still and that the pipe is completely filled with water, see figure 4.9. A change of temperature equal to $\Delta t = 0.02$ is desired for the water. The heat element emits a heat pulse which is of 11 V and 0.5 A, and lasts for 5 seconds. The question is to what volume can the heat pulse provide the desired temperature change?
We assume that the heat pulse is evenly spread into the water and that there exists no heat transfer with the surroundings. Density of water is $\rho_w(21C) = 0.99802 g/cm^3$ and specific heat capacity is $C_p w = 4.184 J/gC$.

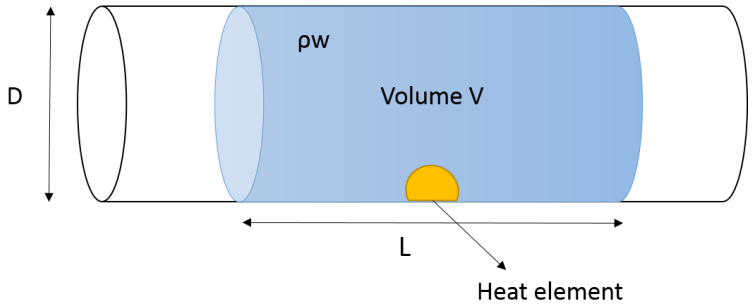

Figure 4.9: Figure of pipe filled with water

The amount of energy that is applied to the fluid from the heat source is calculated from the definitions of electric power:

$$P = U_v I \tag{4.1}$$

where P is electric power in watts, U_v is voltage in volts and I is the electric current in amperes.

$$P = 11.0V \cdot 0.5A = 5.5W$$

$$P = \frac{E}{t} \tag{4.2}$$

where E = energy in joule (J) and t is time in seconds (s).

$$E = P \cdot t = 5.5W \cdot 5s = 27.5J$$

The amount of energy/heat applied is q = 27.5 J.
Heat transfer is given:

$$Q = mC_p\Delta T \tag{4.3}$$

where Q is the amount of heat in joule (J), m is the mass in grams (g), C_p is specific heat capasity of water in J/gram C and ΔT is the change in temperature (C).

$$m = V_p\rho_w \tag{4.4}$$

$$V_p = \pi\frac{D^2}{4}L \tag{4.5}$$

$$V_p = \frac{Q}{\rho_w \cdot C_p \cdot \Delta T} \tag{4.6}$$

In this case the exact volume where the temperature is noticeable is

$$V_p = \frac{27.5J}{0.99802g/cm^3 \cdot 4.184J/gC \cdot 0.02C} = 329cm^3$$

The heat pulse can give a temperature change in a volume equal to 329 cm^3. This is equivalent to a pipe length of 52 cm, when assumptions are taken into account. This is not realistic in relation to the setup used in these experiments, since it is assumed that the temperature change is for the entire volume of the cross-section of the pipe. In the horizontal pipe section with fluid flow, it is desirable that the temperature change occurs in the volume flowing pass and in touch with the heat source and not the entire volume surrounding the heat source. However it is likely to believe that a larger volume is heated up by the heat pulse and that the heat pulse is widely spread. Also one should assume that heat transfer between the surroundings and the experimental setup could be present since the pipes are not insulated and the system is an open system. In addition, the light bulb heats up its surroundings. As long as there exist a temperature difference between the fluid inside the pipes and the ambient temperature, transfer og heat will occur. This is among the reasons why it is desirable with a concentrated heat pulse, so less energy of the applied heat pulse is necessary to measure a change in temperature, as well as a possible decrease in heat transfer.

4.5 Visualization of Heat

By illuminating the area around the light bulb when a heat pulse was applied, it is seemed like a buoyant plume rose from the light bulb. The fluids exhibits density differences due to temperature differences. After adding seeding particles this situation seemed to be more visible. There was a rise of particles above the light bulb and up to the opposite pipe wall, where particles spread out to the sides.

It was desirable to investigate how the heat pulse from the heat source spread into the fluid. By visualizing the heat pulse, one could gain a better understanding of how the heat effects the fluid and what kind of pattern it follows. Among the proposals was application of encapsulated liquid crystals. Thermochromic liquid

crystals, TLC, is widely used for visualization of heat transfer and flow in pipes and fluids. A significant optical characteristic of TLC is the color change with temperature [24]. The crystals reacts to the differences in temperature of the fluid and visualize the heat as a colormap showing different colors for different fluid temperatures. This change in color is repeatable and reversible [25]. Acquisition of these crystals accounted was to time-consuming for this thesis, but application of TLC could be considered for an additional analysis of heat flow.

Several proposals on methods to visualize the heat were examined, but due to limited time and resources, it was finally decided to examine the heat using PIV.

4.5.1 Dynamics of the Heat Source

Static Analysis

In the static analysis there existed no further fluid flow apart from the fluid flow caused by the heat pulse itself.

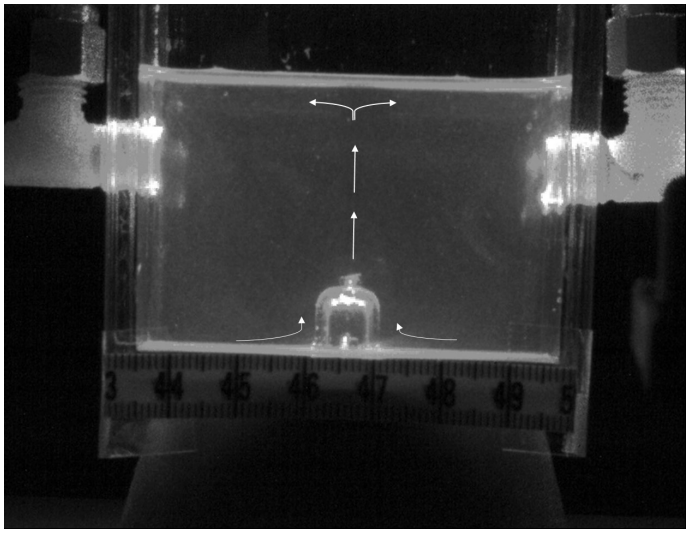

Figure 4.10: Image of heat flow setup with arrows indicating the direction of flow

In figure 4.10 an image frame from this experiment is shown with arrows illustrating the movement of particles. The heat source acts like a jet. It ejects heat from the source in a rectilinear way. It looks like there is a heat rise straight up from the tip of the light bulb and up to the surface of the water. Further it may seem

like the particles deviates from the center and moves away in a circulating motion. Another observation is the particles at the bottom of the container which are swept off the floor and moves in the direction of the warm light bulb. This movement of the seeding particles resemble a convectional motion, as mentioned in section 2.3.1.

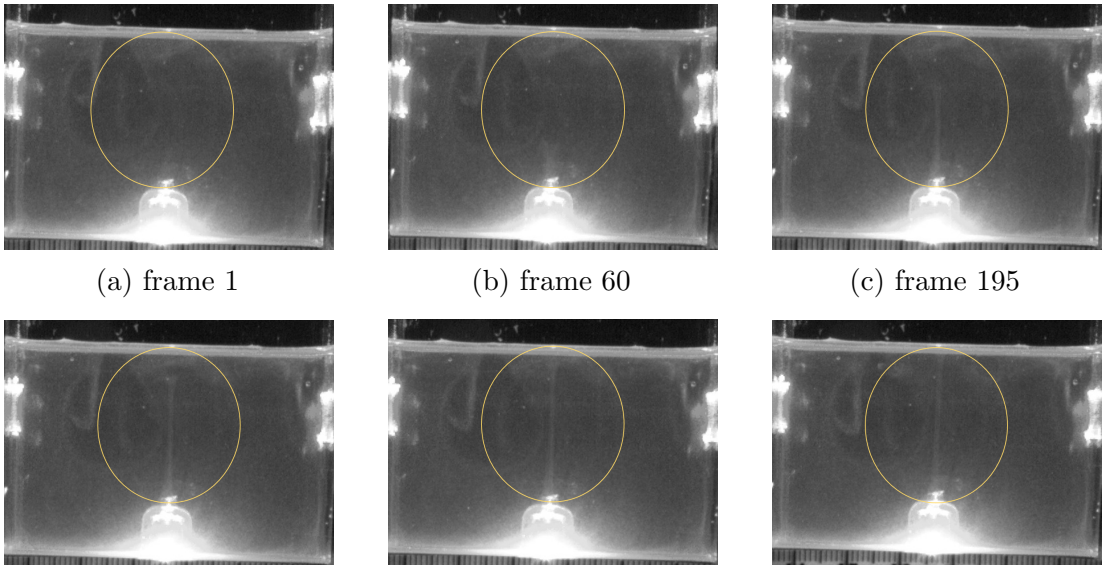

(a) frame 1 (b) frame 60 (c) frame 195

(d) frame 260 (e) frame 310 (f) frame 350

Figure 4.11: Development of heat rise from heat source, impact of heat jet on the water surface. Time between frames is 5 ms.

A sequence of the development of heat rise from heat source is shown encircled in figure 4.11. Six frames visualise how the fluid rises from the heat source when heat is applied. It seems that the geometry of the heat source is reflected in how the heat is distributed in the fluid. A concentrated heat jet rises from the tip of the light bulb, and one should also assume that heat is distributed from across the whole light bulb. As the heated fluid rises as a motion similar to a jet from the tip of the light bulb. It looks like it develops into a heat plume going from the tip of light bulb and up to the interface between fluid and air. As the interface is reached, it seems that the heat jet spreads out on both sides of the center in a counter-clockwise motion.

Results from analysis in PIVlab:

The results from PIVlab is two-dimensional velocity field measurements extracted

from the processed data. Velocity vectors are calculated using image pairs which were taken in a time interval of 5 ms. The velocity magnitude is defined as $A_m = \sqrt{u^2 + v^2}$, where u is horizontal velocity and v is vertical velocity.

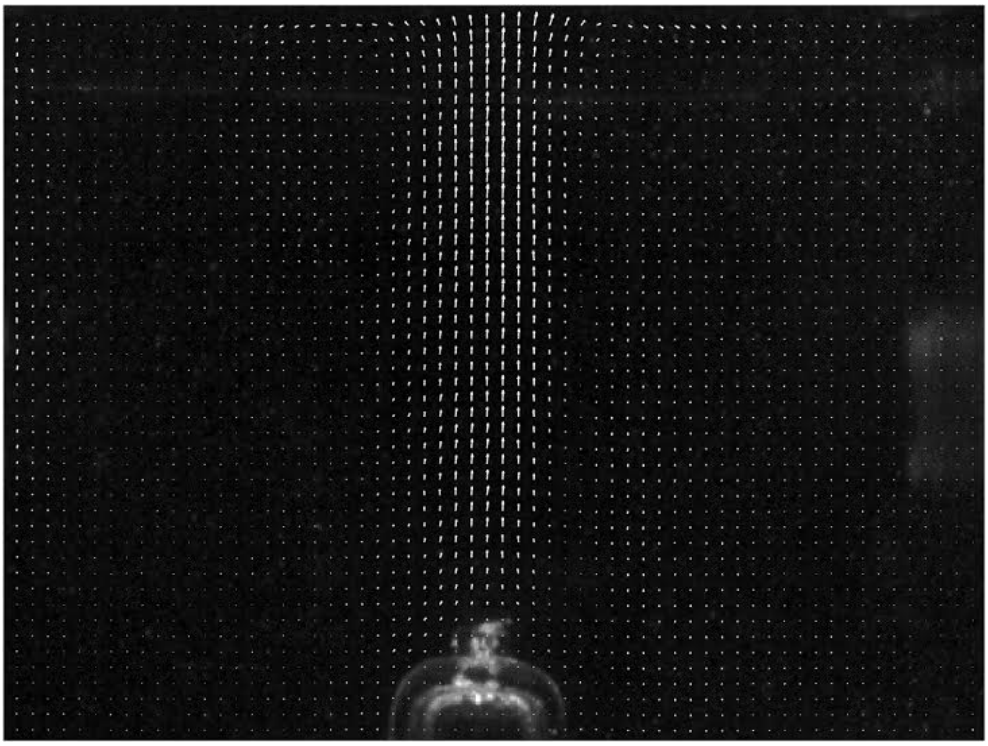

Figure 4.12: Averaged velocity vectors

Figure 4.12 shows the averaged velocity vectors of 400 image pairs which represents 4.0 seconds of recording. The image is extracted from PIVlab and the vectors is seen from the side of the container. The time between images is 5 ms. At the impingement between the heat jet and air it looks from the velocity vectors that there is an elevation of the interface. The average velocity vectors shows how the direction of the fluid changes to a counter clockwise direction. This can also be shown from the u component of the velocity vectors in figure 4.13. In the upper part of this imagea change in direction of the u component can be seen as the direction of the u component are positive in one direction and negative in the opposite direction.

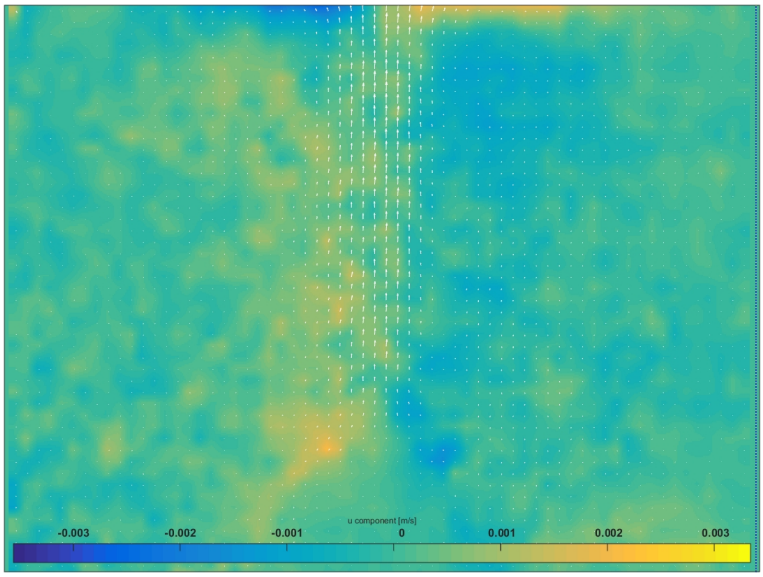

Figure 4.13: u component of velocity vectors

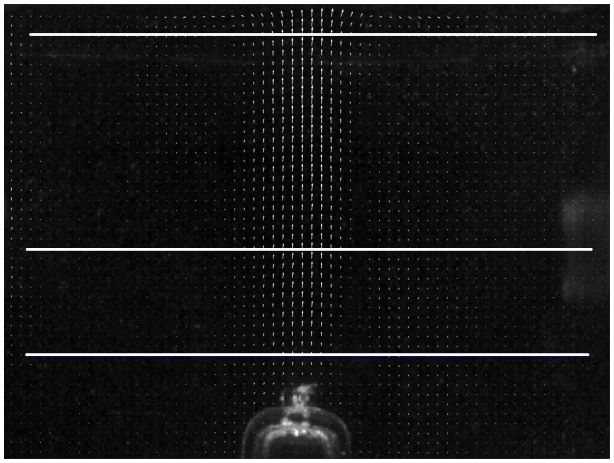

Figure 4.14: Placement of polylines the across the flow in container

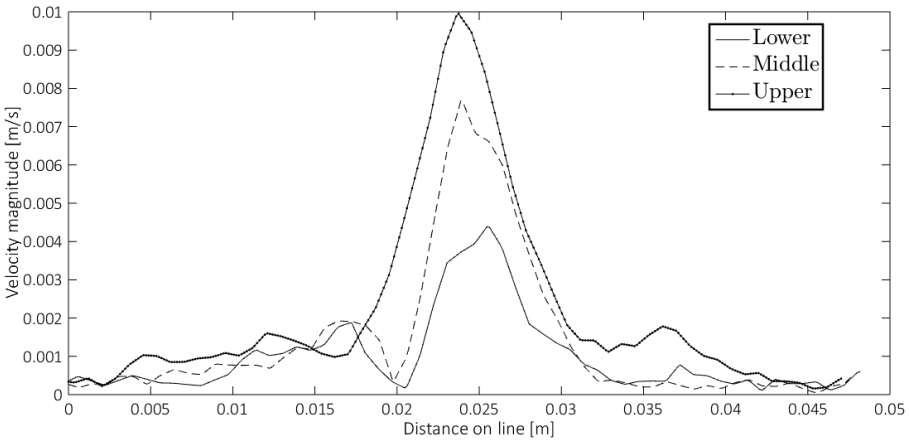

Figure 4.15: Velocity magnitude at lower, middle and upper position above light bulb

The velocity magnitude from the same images across the heat rise is extracted as polylines and plotted in figure 4.15. The results is showing the velocity magnitude across the heat rise in three different positions; lower, middle and upper of the container, as seen in figure 4.14. The velocity in the middle of the plume is higher for all three polyline positions, indicating that the maximum velocity is in the center of the plume.

Dynamic Analysis

In the dynamic analysis, the fluid flows through the container and creates a system more similar to the horizontal setup. An inline pump was installed to control the flow rate of in a loop through the container, as mentioned in section 3.2.2. Since the flow rate was controlled by voltage readings a calibration of the pump was necessary to measure the flow rate in cm^3/s. This was done using a Sensirion SLQ-QT500 flow meter. The results from this is shown in Appendix C. The pump rate used were 0.35 cm^3/s and 1.50 cm^3/s. The container was completely filled with fluid during these experiments, to avoid effects of compressible air.

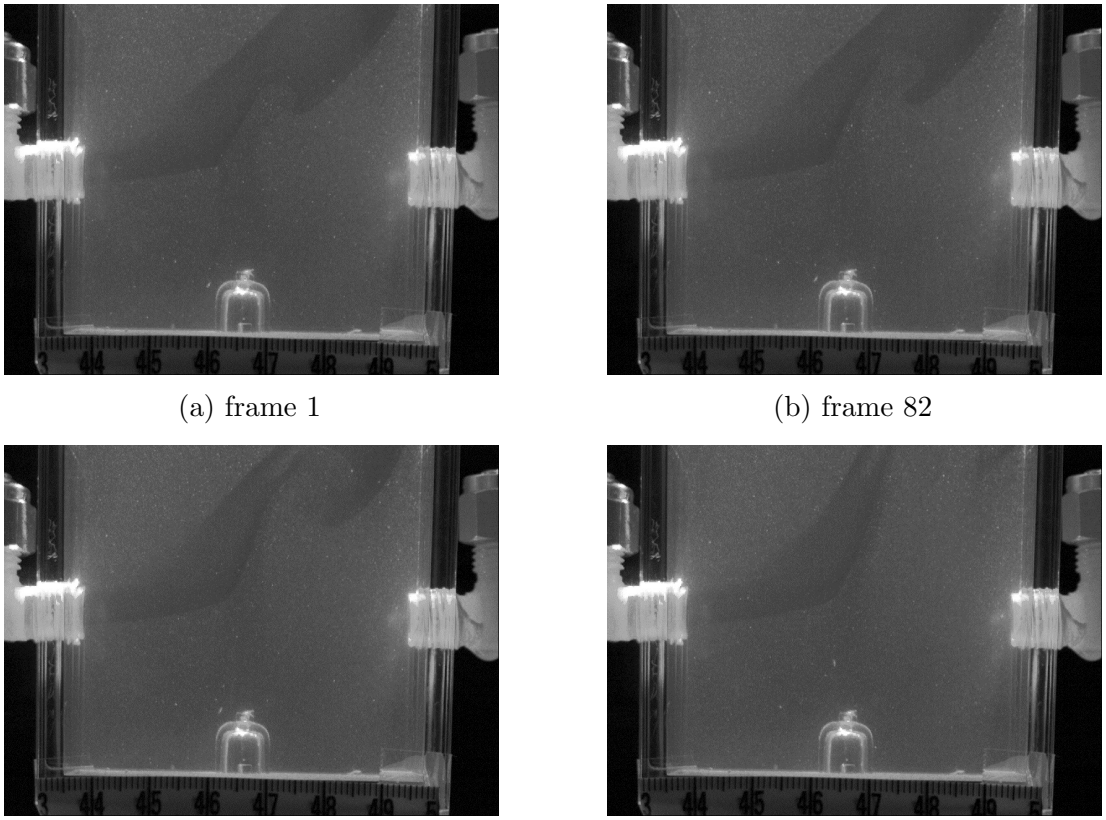

(a) frame 1

(b) frame 82

(c) frame 166

(d) frame 366

Figure 4.16: High-speed images of crossflow between heat jet and crossflow in container

Figures 4.16 shows the dynamics in fluid when a heat pulse is applied to a flowing system. Development of a collision between a heat jet and a crossflow. Initially the flow jet is apparent in the container. The heat dynamics caused fluid rising in a jet-like manner, this was shown in figure 4.12. When the continuous heat jet reaches the crossflow, the shape of the heat jet is changed into a swirl like formation on the exit side of the crossflow.Heat jet intensity seems to be higher than the crossflow velocity. The heat jet fingers inside the crossflow and appears to be amplified. A vortex ring-like structure is formed and simultaneously deviation of the crossflow is observed. This amplification deviates the crossflow and the two jets collide and the mushroom-like structure is formed at the interface. At a late time the vortex increases in size and diffuses coalescences with the surrounding fluid.

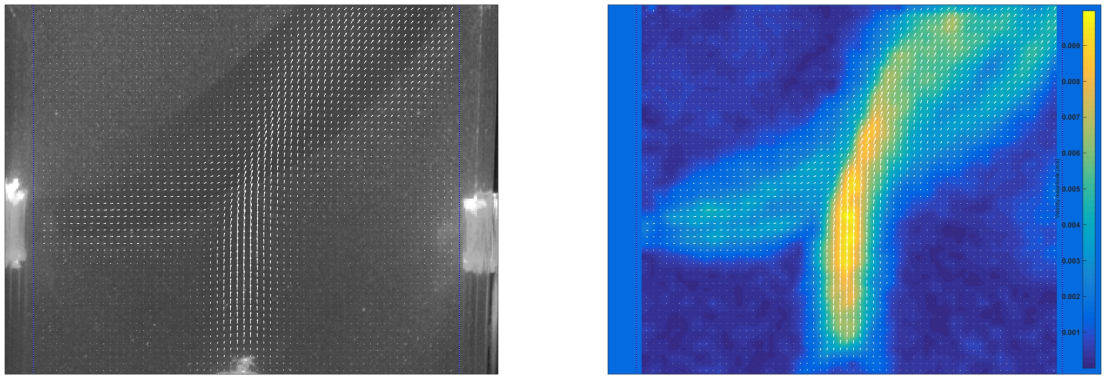

(a) Average velocity vectors (b) Average velocity magnitude

Figure 4.17: Figure of colliding jets in container shown as extracted velocity vectors and velocity magnitude

Figure 4.17 is the results of a PIV analysis of the two jets colliding as seen in figure 4.16. The analysis is conducted on 200 image pairs with the time between image frames equal to 5 ms. image a the average velocity vectors are shown. The velocity pattern shows two jets colliding in the center of the image. In image b the mean velocity magnitude of the same image pairs are shown. It is clearly seen from the velocity magnitude that the heat jet has higher velocity than the crossflow.

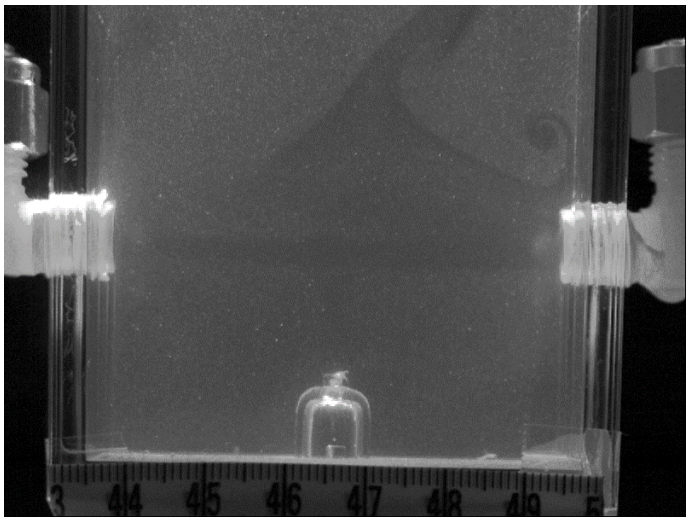

Figure 4.18: Image of flow pattern of colliding jets after flow rate is increased

Afterwards, the flow rate was increased so there was flow through the container. The flow pattern indicated clearly how the crossflow went straight through the container, the heat jet was not as easily seen. Figure 4.18 is taken the moment

the flow rate was increased, it is shown how the fluid flows through the container.

Other Observations

The purpose of using a pump was to imitate crossflow in pipes. In pipes fluid flow unilaterally straight, and the heat jet impinges on it. To have information on how the heat is spread with help from the crossflow, dynamic analysis was performed. However, going from static conditions in the container to dynamic an observation was made. Initially the flow into the container started at a flow rate of 0.35 cm^3/s.

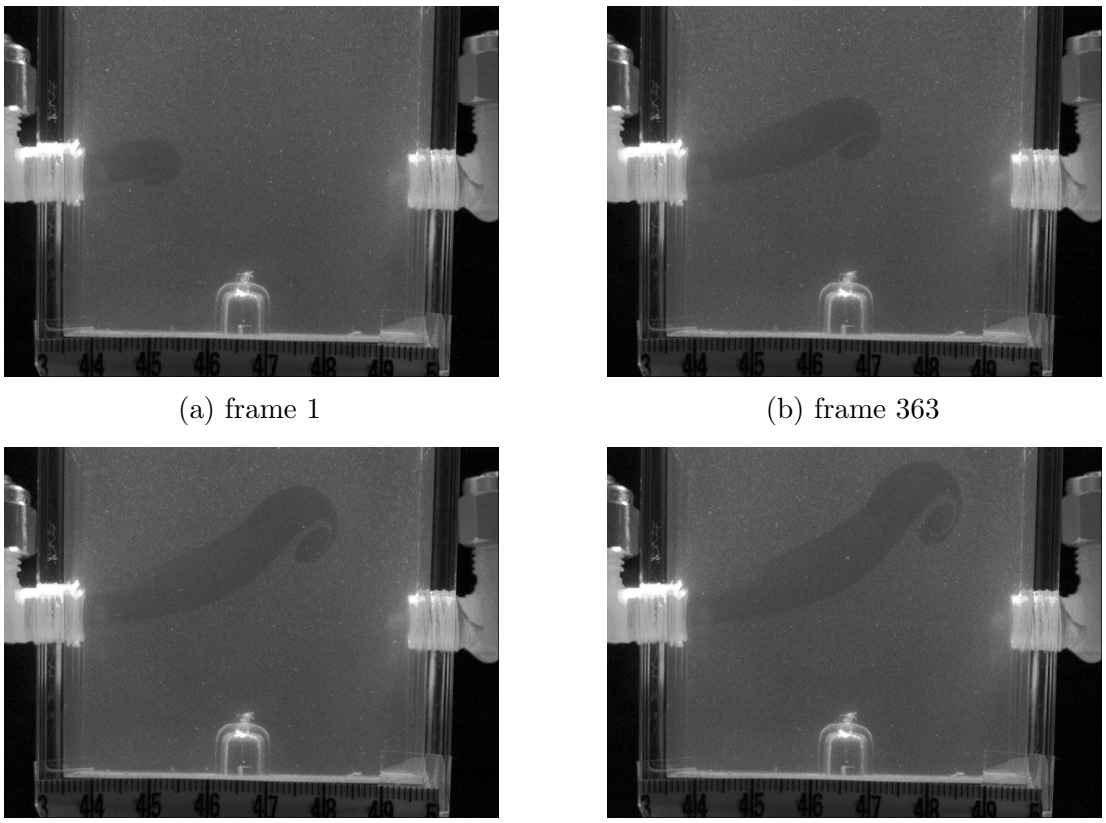

(a) frame 1

(b) frame 363

(c) frame 718

(d) frame 799

Figure 4.19: Initial flow into container when circulation is started. Time between frames is 5 ms.

In figure 4.19 a sequence of the initial flow into the container is given. Prior to this experiment the container was completely filled. Initially as the fluid started to flow into the container a round shape was observed. This shape developed into a jet with similar shape as a mushroom. On the one side a counter-clockwise pattern

was present. A possible reason for this shape could be due to instability between shear layers. Instability like this occurs in situations where velocity difference across the interface between two fluids of different density exists. The fluid with the highest density enters the container and shear the interface with the fluid of lower density inside the container.

4.6 Temperature Measurement

The initial idea was to place the temperature probes inline with the pipe wall. But there a problem with the conducting wire was discovered. The temperature probes and the first centimetre of wire were placed inside the pipe because the Pasco equipment are highly sensitive. The heat conducted by the wire is registered by the temperature probe. These registrations were small and irrelevant compared to ordinary temperature registrations. But since the sensitivity of these sensors is very important, they need to be taken care of.

The wires could have been placed as earlier, outside of the pipe, the temperature change would have been registered. But as the temperature sensors also can be used to give a representative measurement of not only change in temperature but also the temperature of the fluid inside the system. It was therefore decided to include some length of the wires directly into the fluid. In larger systems it could be possible to isolate the wires from the outside of the pipe. This effect could then be minimized and only the temperature probe could disturb the fluid flow.

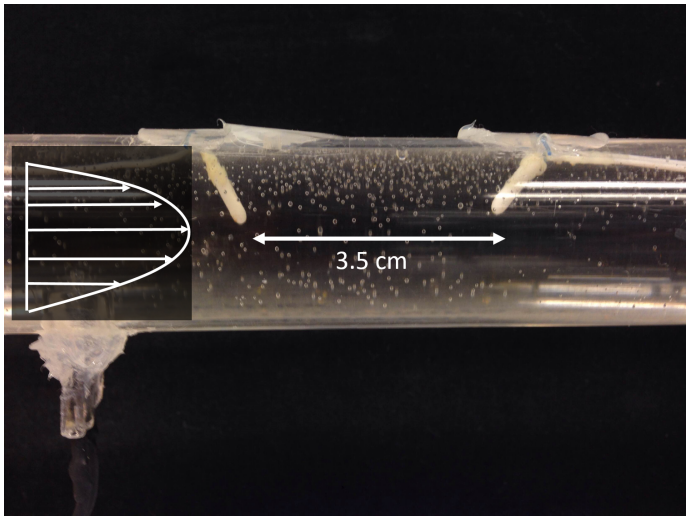

Figure 4.20: Image showing the placement of temperature probes in horizontal pipe setup.

The probes were not placed in line with each other, to prevent one probe shading heat stream to the other. As seen in figure 4.20 the distance between temperature probe tips in this setup was 3.5 cm. They were also placed a short distance from the pipe wall so that they were approximately positioned in the area of average flow rate shown in the velocity profile of laminar flow. One can not assume fully laminar flow, as the heat source and temperature probes are intrusive of the flow. If the probes were positioned in the area of fully developed laminar flow, the heat pulses could be quickly recorded assuming that the heat stream was sent in the same area of the flow.

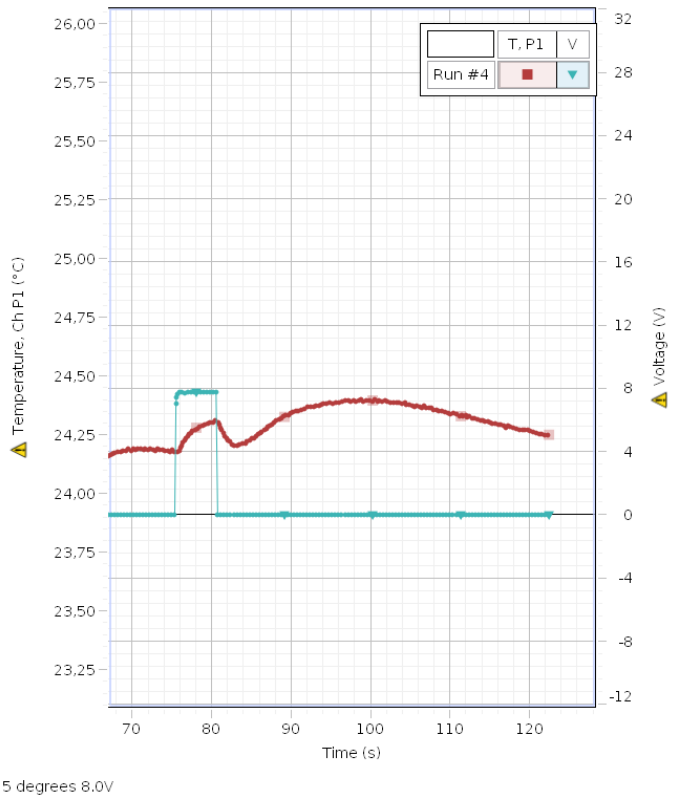

Figure 4.21: Plot extracted from Capstone showing the heat registration of sensor 1 along with the voltage of the light bulb

Instantly after a heat pulse is applied to the fluid an observation is made in the temperature measurements conducted by sensor 1. A subplot extracted from Capstone is showing temperature measurements of sensor 1 and the measured voltage of the heat source, figure 4.21. Temperature of sensor 1 is red and the voltage of the heat source is given in blue. The temperature started to increase although the heat source was turned off. The temperature of sensor 1 is increasing for a while after the heat pulse is applied. Thus effect was not seen for sensor 2. It seemed as if a second pulse of heat was applied to the fluid at the exact moment where the light bulb was shut off. An interpretation is that it could be a response from a convective cell formed by the heat pulse. And that the secondary heat pulse is the next rotation of the cell. It should be mentioned that the distance between the heat source and sensor 1 is short enough it is recorded. As mentioned in section 2.3.1, convective cells are circulating motions due to differences in temperature, which possibly appears in this pipe setup. For higher flow rates, this effect of increasing temperature is not seen.

Even though the Fast Response Temperature Probes from Pasco was highly sensitive, the problem with conductive wire seems to have a negative effect. In a further development of this method alternative temperature sensors is necessary to consider. An alternative could be to use a Pt-element for measuring temperature accurately. These sensors are reliable with high degree of accuracy in measurements for the temperature range relevant in these experiments.

4.7 Placement of Sensors and Heat Source

In order to gain optimal recording of heat pulses using Pasco equipment the distance between the heat source and the temperature is considered. The distance should be of a size that the heat pulse reaches sensor 2 and does not diffuse before reaching it. If the distance between the two sensors are too short, there will be no difference in time of recording heat pulses. The placement has to be adapted in every setup this method is applied. The current experimental setup was built to check the concept of sending heat pulses and registering a time shift, in doing so several parameters was controlled in order to have optimized registration of heat peaks. In addition to the placement of equipment, voltage strength of heat pulse and rate of inflow is adapted during these experiments to gain optimal recording of heat peaks.

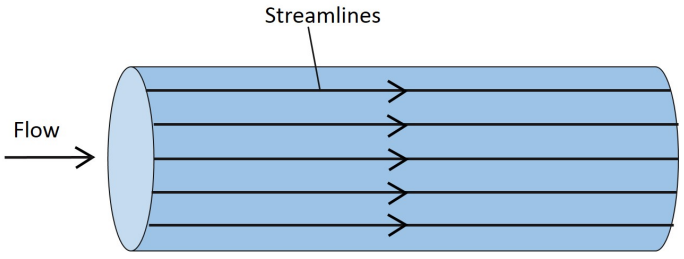

Figure 4.22: Illustration of streamlines in pipe with tubular surface

A possibility to ensure that very low velocity measurements are representative for the fluid flow/pattern in the pipe is to have tubular surface which will form the streamlines to flow along, see figure 4.22. By attaching the heat source and temperature sensors to a smaller and thin-walled pipe the flow entering the smaller

pipe will have the same flow pattern as for the rest of the flow. If a setup like this is made, it would be possible to measure the flow at several places in the pipe.

4.8 Pasco Measurement Equipment

Measurement of experimental data is conducted mostly by Pasco measurement equipments. The sensors used is Absolute Pressure/Temperature Sensor and Voltage-Current Sensor.

However, the conducting wire connected to the temperature probe was a source of uncertainty. An attempt to minimize this effect was by including the wires into the pipe. A possible result of this solution is that larger disturbances of the flow will occur. This is not desirable for a system were concentrated heat pulses should be effectively applied to the flow.

Since the Pressure measurements were highly sensitive to the surroundings, even the slightest little change was recorded. Figure 4.4 describes these artefacts. Vibrations from the surroundings were registered even when the distance from the sensor was considerable. Even though it was possible to use the absolute change in pressure as an indicator for fluid flow, it was not optimal.

The sampling rate using Pasco is up to 100 Hz, and the sensors have a high resolution which results in very accurate measurements. The equipment is suitable for the application in these kind of experimental work. The sensor shows great response to the measurements with a high resolution.

Conclusion

The current study presents feasibility studies in development of thermal based flow measurement technique for very low flow velocities. These were performed in both vertical and horizontal setup. Pasco equipment was used in determination of temperature and pressure. These instruments were fast and highly sensitive. High-speed video and PIV were used to visualize and quantify flow dynamics induced by the heat source.

Based on the experimental work and analysis in PIV, the following conclusions can be drawn:

- Feasibility studies shows that distinct heat pulses in the flow is necessary to be able to calculate the time shift between the temperature sensors using cross correlation function. It is reasonable to conclude from these studies that the best thermal performance can be achieved if a more concentrated heat power is placed in the center of the pipe to minimize diffusion of heat. Based on small-scale laboratory works location of the measurement equipment was decisive in terms of getting best possible registrations of heat pulses. This may yield a considerable better registration of time shift because velocity measurements is dependent on registration of clear and distinct heat peaks.
- Based on the visual analysis of heat source in static environments, it was observed that the heat pattern was a jet rising straight from the top of the heat source and developing into a convectional motion. From the quantification of the heat dynamics the measured velocity magnitude was maximum in the center of the jet.

- Additional experiments show that the collision of crossflow and jet rising from the heat source resulted in a mushroom-like vortex structure.
- Flow meter from Sensirion appeared to be a good candidate in flow measurement for very low flow velocities. Equipment from Pasco performed satisfactory during the experiments. It was fast, highly accurate and easy to use. Flow meter from Sensirion was used in calibration and gave satisfactory results although uneven time series of the data was obtained. These data was further analysed.
- The main goal for studying thermal based flow measurement technique for very low flow velocity is the requirement of its application in the NORTH project. Hence the results from this study should be tested for such applications.

References

[1] Stefan Rahmstorf. Thermohaline ocean circulation. Encyclopedia of Quaternary Sciences, Elsevier, 2006.

[2] Carl Wunsch. Thermohaline loops, stommel box models, and the sandstrom theorem. Tellus, 2004.

[3] Dantec Dynamics. Measurement principles of piv, 2013. URL `http://www.dantecdynamics.com/measurement-principles-of-piv`. [Online; accessed 20-February-2016].

[4] The Engineering Toolbox. Thermal conductivity of some common material and gases. URL `http://www.engineeringtoolbox.com/thermal-conductivity-d_429.html`. [Online; accessed 30-May-2016].

[5] Hiroyoshi Koizumi. A micro flowmeter based on the measurement of a diffusion temperature rise of a locally heated thermal flow in a hagen–poiseuille flow. Flow Measurement and Instrumentation 34: 19–26, Elsevier, 2013.

[6] Rune W. Time. Two-phase flow in pipelines - course compendium. University of Stavanger, 2009. Course compendium.

[7] Bjerknessenteret. The north, 2016. URL `http://www.bjerknes.uib.no/prosjekt/north`. [Online; accessed 20-February-2016].

[8] Whitehead. Abrupt transitions and hysteresis in thermohaline laboratory models. Tellus, 2004.

[9] Y.A.Cengel et.al. *Fundamentals of Thermal-Fluid Sciences*. McGraw-Hill, New York, 4th edition, 2012.

[10] Wikipedia. Advection — wikipedia, the free encyclopedia, 2016. URL `https://en.wikipedia.org/w/index.php?title=Advection&oldid=707383943`. [Online; accessed 30-May-2016].

[11] R. E.Sonntag , C. Borgnakke. *Fundamentals of Thermodynamics*. Wiley, Hoboken, N.J, 7th edition, 2009.

[12] Encyclopedia Britannica. Turbulent flow, 2016. URL `http://global.britannica.com/science/turbulent-flow`. [Online; accessed 30-May-2016].

[13] Massachusetts Institute of Technology MIT. Basics of turbulence flow. Online. URL `http://www.mit.edu/course/1/1.061/OldFiles/www/dream/SEVEN/SEVENTHEORY.PDF`. [Online; accessed 25-05-2016].

[14] Bathsheba Kerubo Menge. Analysis of turbulent flow in a pipe at constant reynolds number using computational fluid dynamics. Jomo Kenyatta University of Agriculture and Technology, 2014.

[15] J.B. Franzini E.J.Finnemore. *Fluid Mechanics with Engineering Applications*. McGraw-Hill, Boston, 10th edition, 2002.

[16] John P. Bentley. *Principles of Measurement Systems*. Pearson/Prentice Hall, Harlow, 4th edition, 2005.

[17] David S. Stoffer , Robert H. Shumway. *Time series analysis and its applications: With R Examples*. Springer New York, New York, 2011.

[18] L.M. Gratton et al. Very fast temperature measurement with a thin lamp filament. Physics Education – IOPscience. 2010; 31(4): 933-942., 2012.

[19] Dantec Dynamics. Particle image velocimetry, 2013. URL `http://www.dantecdynamics.com/particle-image-velocimetry`. [Online; accessed 20-February-2016].

[20] M.J. Chern et al. Performance test and flow visualization of ball valve. Experimental Thermal and Fluid Science, 31 (6), pp. 505–512, 2007. Article.

[21] Pasco. Pasport fast response temperature probe (3 pack) p-2135, 2016. URL `https://www.pasco.com/prodCatalog/PS/PS-2135_pasport-fast-response-temperature-probe-3-pac/`. [Online; accessed 5-June-2016].

[22] C. Nilsson J. Habainy. Oxidation of pure tungsten in the temperature interval 400c to 900c. Lund University, department of mechanical engineering, 2013.

[23] W. Thielicke and E.J. Stamhuis. Pivlab – towards user-friendly, affordable and accurate digital particle image velocimetry in matlab. Journal of Open Research Software, 2: e30, 2012. software metapaper.

[24] James W. Baughn. Liquid crystal methods for studying turbulent heat transfer. Int. J. Heat and Fluid Flow 16: 365-375, by Elsevier Science Inc., 1995.

[25] T.A.Kowalewski J.A.Stasiek. Thermochromic liquid crystals applied for heat transfer research. Opto- Electronics Review 10(1), 1–10, 2002. Article.

Specifications

A.1 Pasco Measurement Equipment

Pasco Absolute Temperature/Pressure Sensor PS- 2146

	Pressure (kPa)	Temperature (degrees Celsius)
Range	0 - 700	0 - 70
Accuracy	±2	±0.5
Resolution	0.1	0.0025
Repeatability	1	0.01

Online source: https://www.pasco.com/file _ downloads/product_ manuals/

Pasco Voltage Current Sensor PS - 2115

Voltage Range:

± 10 V

± 50 mV at 10 V accuracy

5 mV resolution

Current Range:

± 1A

± 5mA at 1 A accuracy

500 μ A resolution

Maximum sampling rate 1kHz

Maximum voltage 10 V maximum common mode voltage

Maximum input: current 1.1 A and voltage 30 V

Online Source: https://www.pasco.com/prodCompare/voltage-current-sensors/index.cfm

A.2 Manson SPS-9602 Swithcing Mode Power Supply

Variable Output Voltage: 1- 30 V

Total Rated Output Current: 30A

Meter accuracy: $\pm 1\% + 1 count$

Efficiency: $> 85\%$

Online source: http://www.manson.com.hk/products/detail/67

A.3 Basler

Camera Model: acA800-510uc USB 3.0

C- mount

Resolution 80px x 600px

Frame rate 511 fps

Pixel Size horizontal/vertical 4.8 μm x 4.8 μm

Camera Lens: C125- 1620-5M

Focal lenght 16 mm

F-stop settings F2.0 - F22

Online Source: http://www.baslerweb.com/en/products/

A.4 Sensirion Flow Meters

Sensirion SLS - 1500 Liquid Flow Meter

Full scale flow rate 40 ml/min

Accuracy 5 % of measure value

Repeatability 0.5 % of measured value

Flow detection response time 20 ms

Operating temperature +5 - +50 degrees Celsius

Operating pressure 12 bar

Sensirion SLQ - QT500 Liquid Flow Meter

Full scale flow rate 2000 micrometer/second

Accuracy below full scale 5 % of measure value

Repeatability below full scale 0.5 % of measured value

Flow detection response time < 50 ms

Operating temperature +5 - +50 degrees Celsius

Operating pressure 12 bar

Online Source: https://www.sensirion.com/

MATLAB Scripts

B.1 vdosplit.m

```
%%Extracting & Saving of frames from a Video file through Matlab
    Code%%
clc;
close all;
clear all;
% Tested 8.10.2015 by Benja

% assigning the name of sample avi file to a variable
%filename = 'Video.mov';
%filename = 'Video-2.mov';
%filename = 'Video-5.mov';
filename = 'Video-6.mov';

%reading a video file
mov = VideoReader(filename);

% Defining Output folder as 'snaps'
opFolder = fullfile(cd, 'snaps');
%if  not existing
if ~exist(opFolder, 'dir')
%make directory & execute as indicated in opfolder variable
mkdir(opFolder);
end
```

```
%getting no of frames
numFrames = mov.NumberOfFrames;

%setting current status of number of frames written to zero
numFramesWritten = 0;

%for loop to traverse & process from frame '1' to 'last' frames
for t = 1 : numFrames
currFrame = read(mov, t);    %reading individual frames
opBaseFileName = sprintf('%3.3d.png', t);
opFullFileName = fullfile(opFolder, opBaseFileName);
imwrite(currFrame, opFullFileName, 'png');   %saving as 'png' file
%indicating the current progress of the file/frame written
progIndication = sprintf('Wrote frame %4d of %d.', t, numFrames);
disp(progIndication);
numFramesWritten = numFramesWritten + 1;
end      %end of 'for' loop
progIndication = sprintf('Wrote %d frames to folder "%s"',
    numFramesWritten,opFolder);
disp(progIndication);
%End of the code

% Read more: http://www.divilabs.com/2013/11/extracting-saving-of-
    frames-from-video.html#ixzz3nuCp9nS4
```

B.2 conv_gray.m

```
% Program to convert RGB frames to grayscale
% Preparations of PIV analysis
% 2th May 2016 Marta Ovstebo
% Starts with loading the image frame, then convert the RGB into
    grayscale
% and change the filename into a number.

clc
clear all
```

```
% Specify the folder where the files are:
% myFolder = 'F:\documents\Marta  vsteb \Convert to grayscale';
% noframe = 100; % Total number of frames to analyse

% The counter i has to be changed while converting rgb to grayscale:
% i = 1:1:10 and change Pname eg.000' and imwrite'000'
% i = 10:1:100 Pname eg. 00' and imwrite '00'
% i = 100:1:1000 Pname eg. 0' and imwrite '0'
% i = 1000:1:noframe Pname eg, ' an and imwrite ''

for i = 1000:1:6660
    Pname = strcat('acA800-510uc__21763331__20160502_035501482_',
       num2str(i),'.bmp');
    Read_P = imread(Pname);
    Con_P = rgb2gray(Read_P);
    imwrite(Con_P, [ int2str(i),'.bmp'],'bmp'); %(converted frame,
       new filename, value)
end
```

B.3 Marta_averaging_1.m

```
clc
clear
close all;
RESULTS = [];
Umean=[];

% Reading excel file (from Data Acquisition)
S=1;
E=10640;
% Excel name
filename = 'Marta 13 april 2016 - 4.csv' % Pasco log file - Excel


% Scanning the excel file
% [NUM,TXT,RAW] = xlsread(filename,sheet);
[NUM,TXT,RAW] = xlsread(filename);
```

```
val = NUM;

% Computing variables
Time = val(S:E,2);
U=val(S:E,3);
Umean = mean(val(S:E,2));        %unit (m/s)

Tmax = 880 % Hvis Tmax settes stoerre enn siste verdi faller de
    siste verdiene
          % til negative verdier,siden vi  g r  forbi input grensen
dt=1.0
Tmin = dt;
Tsnew = Tmin:dt:Tmax;
% Uspline = spline(Time,U,Tsnew);
Uinterp1 = interp1(Time,U,Tsnew,'nearest');

U0 = 20.7;
t0 = 43.3;
Uteori1 =U0*exp(-(Time-t0)/135);

figure(1);
plot(Time,U)
hold on
%plot(Time,Uteori1,'-k')
title('Time series of velocity - uneven spaced')
xlabel('t(s)')
ylabel('U(t)- ml/min')

% figure(2);
% plot(Tsnew,Uspline)
% title('Cubic spline interpolated time series of velocity')
% xlabel('t (s)')
% ylabel('Uspline(t)')

U0 = 20.7;
t0 = 43.3;
Uteori =U0*exp(-(Tsnew-t0)/135);

figure(3);
```

```
plot(Tsnew,Uinterp1)
hold on
title('Interpolated (nearest) time series of velocity - even spaced'
    )
xlabel('t (s)')
ylabel('Uinterp1(t)- ml/min')
%plot(Tsnew,Uteori,'-k');
```

B.4 Flow_ccf _june_RWT.m

```
% Cross correlation of low velocity fluid flow %
% Program for cross correlation of data from experiments executed
    with flow
% in tube, where two temperature probes are placed above a heating
    source.
% The experiments is performed with a sampling rate of 100 Hz, dt =
    1e-2.
 clc
 clear all
 clf

% Upload data from Excel:
 filename = 'testdataccf.xlsx';          % filename
 sheet = 1;
 xlRange = 'A4:E8000';              % choose cell position of data
 subsetA = xlsread(filename,sheet,xlRange);

% Chose data from the temperature dataset to be analyzed:
 time =  subsetA(:,1);               % set position of time
 dt=time(2)-time(1)
 sensor1 = subsetA(:,2);             % set sensor 1 position
 sensor2 = subsetA(:,3);             % set sensor 2 position
 Lengde = length(time)


 % Set amount of data to analyze - from L1 to L2
 L1 = 100
```

```
 L2 = 1600

 %%% Cross correlation function %%%
Tid =  time(L1:L2);
Flytt=0 %Play parameter for an artificial time shift to check if the
    "tshift" follows
Sensor1 = sensor1(L1+Flytt:L2 + Flytt);
max1=max(Sensor1)
min1=min(Sensor1)
Sensor1 = (Sensor1 - min1)/(max1-min1) %Scale signal to be between 0
    and 1

Sensor2 = sensor2(L1:L2);
max2=max(Sensor2)
min2=min(Sensor2)
Sensor2 = (Sensor2 - min2)/(max2-min2) %Scale signal to be between 0
    and 1

% Plot of temperature in time series
 figure(1)
 plot(Tid, Sensor1, '-r')
 hold on
 plot(Tid, Sensor2)
 xlabel('Time');
 ylabel('Sensor signal');
 legend('Sensor 1','Sensor 2',1);
 title('Temperature probes - time series')
 hold off

% Plot the last peaks separately
p1=1000
p2=1600
S1 = sensor1(p1:p2);
S2 = sensor2(p1:p2);
T  = time(p1:p2);
ma1=max(S1)
mi1=min(S1)
ma2=max(S2)
mi2=min(S2)
```

```
S1 = (S1 - mi1)/(ma1-mi1) %Scale signal to be between 0 and 1
S2 = (S2 - mi2)/(ma2-mi2) %Scale signal to be between 0 and 1


 figure(3)
 plot(T, S1, '-r')
 hold on
 plot(T, S2,'-b')
 xlabel('Time');
 ylabel('Sensor signal');
 legend('Sensor 1','Sensor 2',1);
 title('Temperature probes - time series')
 hold off


N = length(Tid);
nb = 70
    for i = 1:nb
        shiftid(i)=i*dt;
        CH=0;
        chref=0;
        for j=1:N - nb -1
        CH = CH + Sensor2(j+i)*Sensor1(j); % Sensor 2 comes after
            sensor 1
                                           % so a "later" time has
                                              to be
                                           % searched for similarity
        chref=chref + Sensor2(j)*Sensor1(j);
        end
        CCF(i)= CH;
    end
  CCF=CCF/chref;

% Plot of cross-correlation function
figure (2)
plot(shiftid,CCF)
xlabel('Time shift(s)')
ylabel('Correlation - CCF (normalized)')
title('Cross correlation function')
```

```
% Finding maximum cross-correlation between signals
Maxccf = max(CCF)
for i=1:nb
    if CCF(i)== Maxccf
        tshift=i       % Time shift
        Timeshift=tshift*dt
    end;
end

%Cross correlate the last peaks in figure3
% ************************************
NN = length(T);
nb = 70
    for i = 1:nb
        shiftid2(i)=i*dt;
        CH=0;
        chref=0;
        for j=1:NN - nb -1
        CH = CH + S2(j+i)*S1(j); % Sensor 2 comes after sensor 1
                                 % so a "later" time has to be
                                 % searched for similarity
        chref=chref + S2(j)*S1(j);
        end
        CCF2(i)= CH;
    end
  CCF2=CCF2/chref;

% Plot of cross-correlation function
figure (4)
plot(shiftid2,CCF2)
xlabel('Time shift(s)')
ylabel('Correlation - CCF2 (normalized)')
title('Cross correlation function - last peak')

% Finding maximum cross-correlation between signals
Maxccf2 = max(CCF)
for i=1:nb
```

```
    if CCF(i)== Maxccf2
        tshift2=i       % Time shift
        Timeshift2=tshift2*dt
    end;
end
```

Calibration of Inline Pump

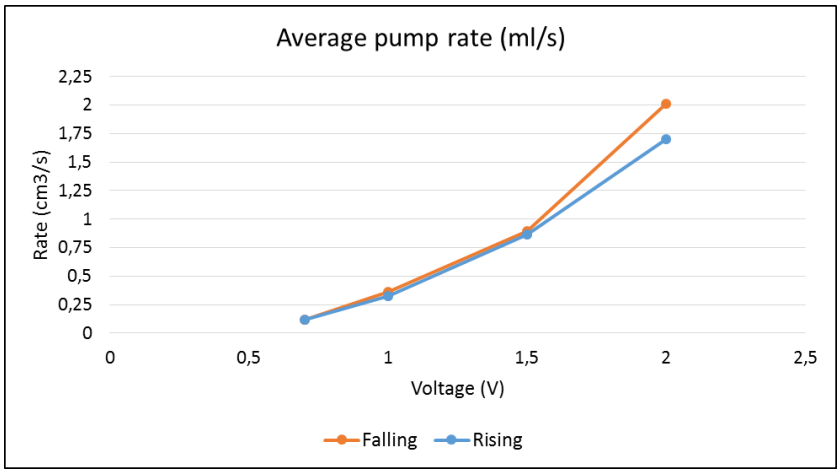

Figure C.1: Measured average pump rate

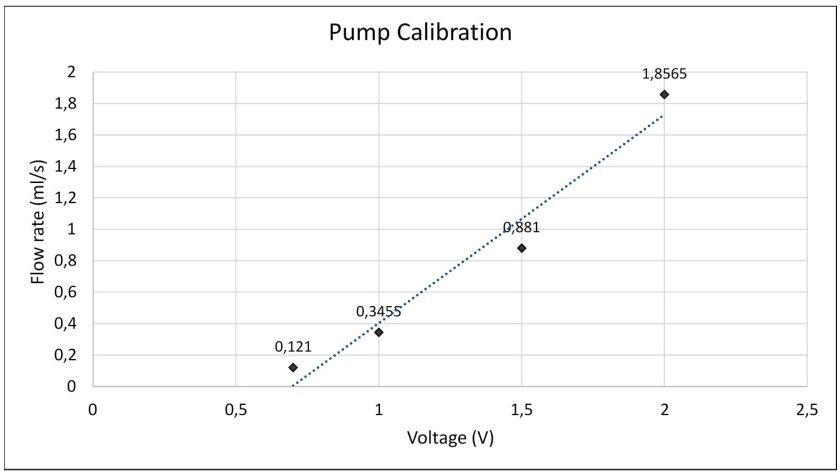

Figure C.2: pump calibration

Trendline equation and R-squared value: $Flowrate = 1.326 \cdot V - 0.9228$

$R^2 = 0.9625$

Illustrations

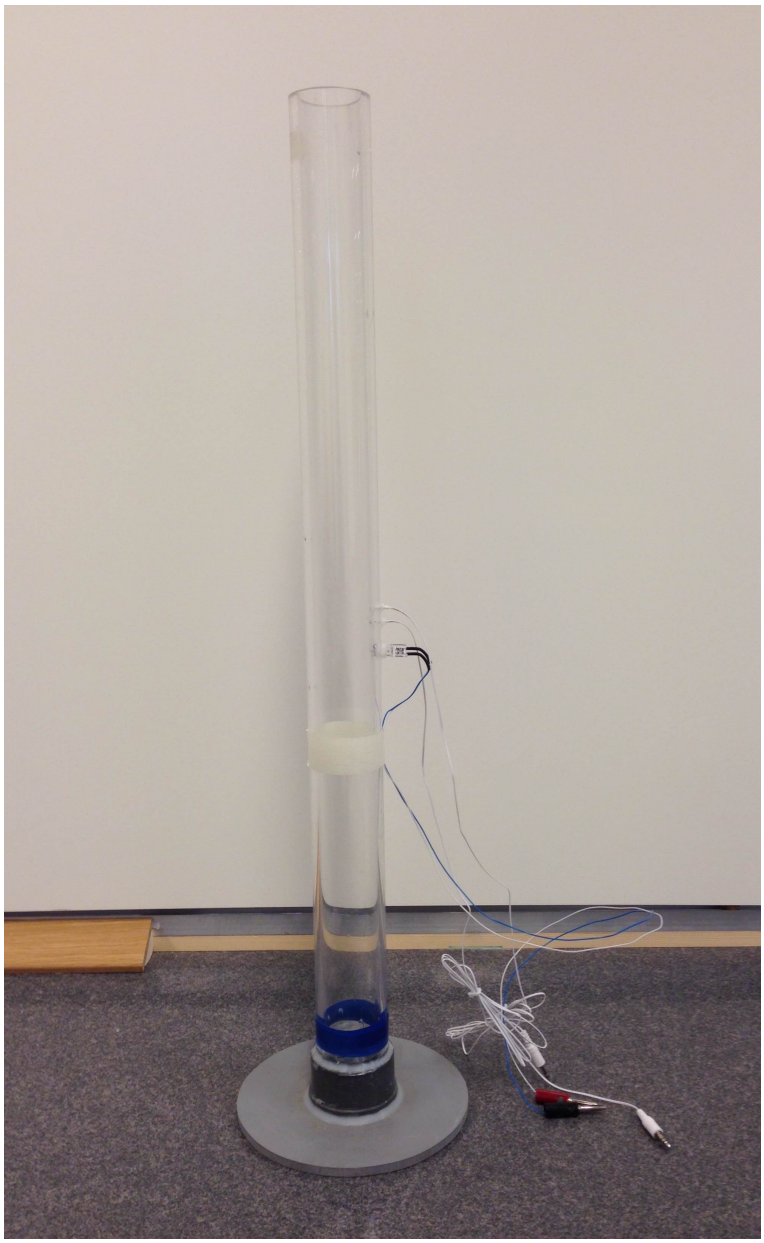

Figure D.1: Vertical Pipe Setup

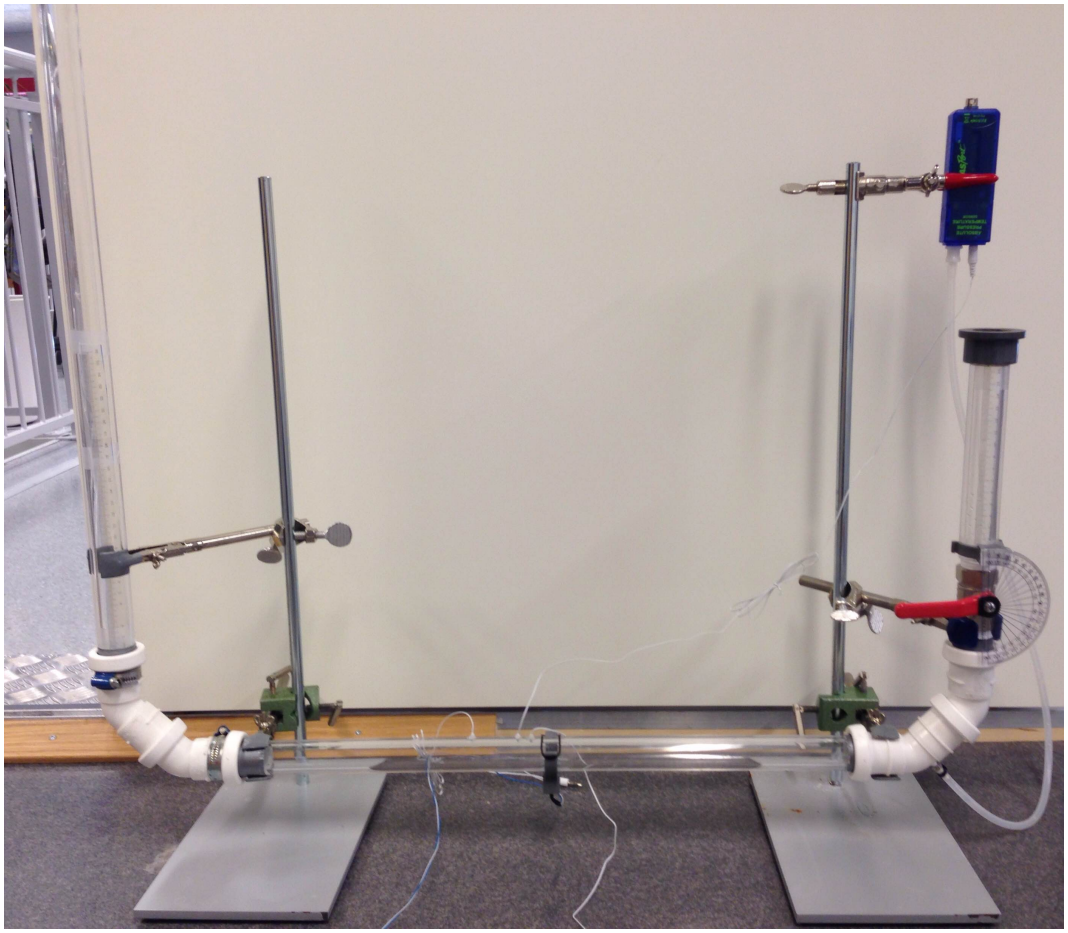

Figure D.2: Horizontal pipe setup

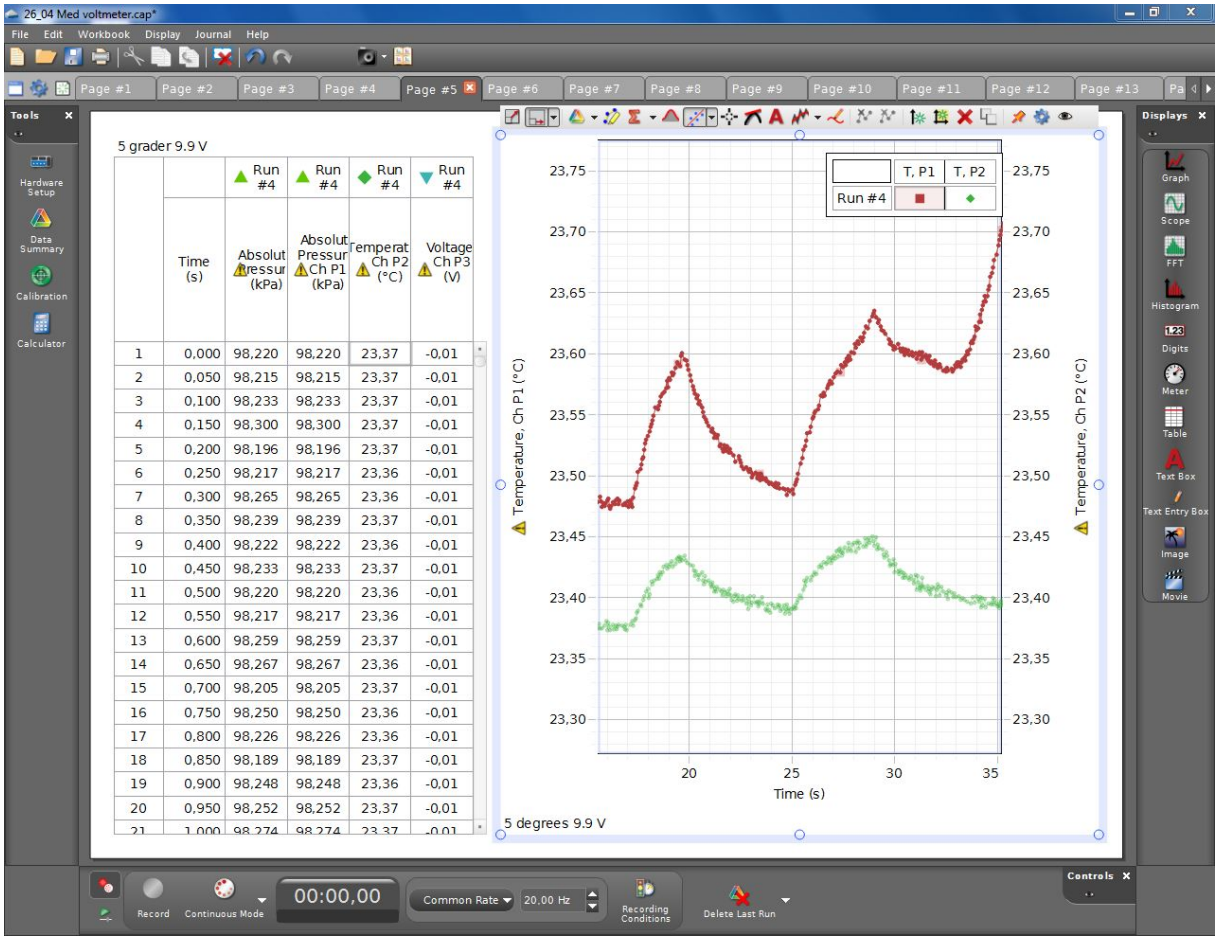

Figure D.3: Screenshot of Capstone